Reconstruction of phylogeographic relationships and evolution of the tundra vole, Alexandromys oeconomus (Rodentia, Cricetidae), based on ancient DNA

Aleksandra Żeromsk, Mateusz Bac, Anna Lemanik, Danije Popović, Magdalena Krajca, Joanna Stoj, Krzysztof Stefaniak, Helen Fewlass, Tatyana Fadeeva, Iva Horáček, et al.

Zoological Journal of the Linnean Society, 2025, **205**(**4**), zlaf154
https://doi.org/10.1093/zoolinnean/zlaf154

OXFORD

Original Article

Reconstruction of phylogeographic relationships and evolution of the tundra vole, *Alexandromys oeconomus* (Rodentia, Cricetidae), based on ancient DNA

Aleksandra Żeromska[1], Mateusz Baca[2], Anna Lemanik[3], Danijela Popović[2], Magdalena Krajcarz[4], Joanna Stojak[5,6], Krzysztof Stefaniak[7], Helen Fewlass[8], Tatyana Fadeeva[9], Ivan Horáček[10], Alexander K. Agadzhanyan[11], Natalia V. Serdyuk[11], Sara E. Rhodes[12], Nicolas Conard[13,14], Emmanuel Desclaux[15], Aurélien Royer[16], Svetlana V. Pavlova[17], Ivan Baláž[18], Leonid Rekovets[19], Claudio Berto[20], Gyozo Horvath[21], Adam Nadachowski[3], Paweł Mackiewicz[1,*]

[1]Faculty of Biotechnology, University of Wrocław, Wrocław, 50-383, Poland
[2]Centre of New Technologies, University of Warsaw, Warsaw, 02-097, Poland
[3]Institute of Systematics and Evolution of Animals, Polish Academy of Sciences, Kraków, 31-016, Poland
[4]Institute of Archaeology, Nicolaus Copernicus University in Toruń, Toruń, 87-100, Poland
[5]Mammal Research Institute, Polish Academy of Sciences, Białowieża, 17-230, Poland
[6]Institute of Genetics and Animal Biotechnology, Polish Academy of Sciences, Jastrzębiec, Magdalenka, 05-552, Poland
[7]Faculty of Biological Sciences, University of Wrocław, Wrocław, 50-335, Poland
[8]Department of Human Evolution, Max Planck Institute for Evolutionary Biology, Leipzig, Germany
[9]Mining Institute Ural Branch, Russian Academy of Science, Perm, Russia
[10]Department of Zoology, Charles University, Prague, Czechia
[11]Borissiak Paleontological Institute, Russian Academy of Sciences, Moscow, Russia
[12]Interdisciplinary Centre for Archaeology and Evolution of Human Behavior, University of Algavre, Faro, Portugal
[13]Senckenberg Centre for Human Evolution and Paleoenvironment, University of Tübingen, Tübingen, Germany
[14]Ur- und Frühgeschichte und Archäologie des Mittelalters, Eberhard Karls University of Tübingen, Tübingen, Germany
[15]Laboratoire départemental de Préhistoire du Lazaret, CEPAM—UMR 7264 CNRS, Nice, France
[16]Université Bourgogne Europe, CNRS, Biogéosciences UMR 6282, 21000 Dijon, France, France
[17]A. N. Severtsov Institute of Ecology and Evolution, Russian Academy of Sciences, Moscow, Russia
[18]Faculty of Natural Sciences, Constantine the Philosopher University, Nitra, Slovakia
[19]Department of Vertebrate Ecology and Paleontology, Wrocław University of Environmental and Life Sciences, Wroclaw, 51-631, Poland
[20]Faculty of Archaeology, University of Warsaw, Warszawa, 00-927, Poland
[21]Institute of Biology, University of Pécs, Pécs, Hungary

*Corresponding author. Faculty of Biotechnology, University of Wrocław, ul. Fryderyka Joliot-Curie 14a, Wrocław 50-383, Poland. E-mail: pamac@smorfland.uni.wroc.pl

ABSTRACT

The Late Pleistocene and Holocene climatic fluctuations profoundly influenced the demographic patterns of many species. Small mammals, particularly rodents, are well-suited for such studies due to their abundance and high environmental sensitivity. A suitable subject is the tundra vole, *Alexandromys oeconomus*, with changing past and present distributions across the Holarctic. Using ancient DNA, we reconstructed its phylogeography and identified 12 main lineages, including extinct lineages, which highlight greater historical variability of this species. Our analyses revealed eastward and westward expansions, extinctions, and lineage replacements driven by climate changes. Originating in Central/Western Asia, the tundra vole expanded around 110 ka (thousand years ago) into Europe, diversifying into multiple lineages. Two migrations from Central Asia to north-eastern Asia occurred at roughly 70 and 16 ka, and preceded the colonization of North America by 11.5 ka. Europe also experienced intense population turnovers, with remigrations into Western Asia. Fennoscandia was colonized three times after 15 ka by two distinct routes. These migrations were tied to climate changes, with population size increasing during warming periods and declining during cooling periods,

Received 13 May 2025; revised 19 August 2025; accepted 18 September 2025

especially during the Last Glacial Maximum. This research provides new findings on how climate and environmental shifts shaped the evolution and distribution of *A. oeconomus*, highlighting the resilience and adaptability of small mammals.

Keywords: ancient DNA; migration; phylogeny; phylogeography; Pleistocene; rodents

INTRODUCTION

The Late Pleistocene and the transition from the last glacial (*c.* 115–11.7 ka) to the Holocene were marked by significant climatic fluctuations playing a crucial role in shaping population dynamics of many species (Blois *et al.* 2010, Brace *et al.* 2012). The rapid environmental changes led to the extinction of entire genetic lineages and the expansion of others (Stewart *et al.* 2010, Cooper *et al.* 2015, Baca *et al.* 2017, Svenning *et al.* 2024), which finally shaped and established the demography of modern species and populations (Niedziałkowska *et al.* 2021, Doan *et al.* 2022, Rabiniak *et al.* 2023, Rabiniak *et al.* 2024, Niedziałkowska *et al.* 2024).

A number of studies about these phenomena are based on ancient DNA and have focused on megafauna, e.g. horses, bears, woolly rhinos, mammoths, reindeer, musk oxen and bison, showing that rapid climate fluctuations shaped their population sizes and ranges but each species responded uniquely to the climatic and anthropogenic pressures (Campos *et al.* 2010, Lorenzen *et al.* 2011, Cooper *et al.* 2015, Niedziałkowska *et al.* 2021, Doan *et al.* 2022, Niedziałkowska *et al.* 2024). Distinguishing between these factors is challenging, but studying species minimally impacted by human activity can provide valuable insights into the relative importance of natural vs. anthropogenic influences. Small mammals, like rodents, are ideal for such studies as they respond faster to environmental changes than megafauna.

Recent studies have demonstrated that rodent population dynamics were mainly driven by climate changes and the availability of open habitats during the Late Pleistocene (Palkopoulou *et al.* 2016, Baca *et al.* 2023b). Species with similar environmental requirements responded similarly to climate change. For example, the time of separation of the three main groups of narrow-headed voles, the European (*Stenocranius anglicus*) and the Asian (*Stenocranius gregalis* and *Stenocranius raddei*), coincided with the time of the separation of the two main groups of collared lemmings, the Eurasian (*Dicrostonyx torquatus*) and North American (*Dicrostonyx groenlandicus* and *Dicrostonyx hudsonius*) (Palkopoulou *et al.* 2016, Baca *et al.* 2020, Lord 2022, Lord *et al.* 2022, Baca *et al.* 2023a, b).

Another interesting species suitable for research on climate and environmental impact is the tundra or root vole, *Alexandromys oeconomus* (Pallas, 1776), which is widely distributed in the Palearctic from western Fennoscandia and north-eastern Germany, through the Northern European Plains and Siberia to the Kamchatka Peninsula and extending into the Nearctic in Alaska and western Canada (Shenbrot and Krasnov 2005). Isolated relict populations in Europe are still present in the Netherlands (Ligvoet and van Wijngaarden 1994) and western Hungary (Gubányi *et al.* 2009, Thissen *et al.* 2015). This species was abundant and frequently found in Pleistocene fossil assemblages (Nadachowski 1989, Maul and Markova 2007, Berto and Rubinato 2013, Banuls-Cardona *et al.* 2014, Garcia-Ibaibarriaga *et al.* 2015, Markova and Puzachenko 2018, Sese *et al.* 2018, Krokhmal' *et al.* 2021, Krokhmal' *et al.* 2023, Stefaniak *et al.* 2023, Popova *et al.* 2025).

The tundra vole belongs to the Arvicolinae subfamily in the Cricetidae family. Based on morphological studies, it was previously assigned to the genus *Microtus* Schrank, 1978 and the subgenus *Pallasiinus* Kretzoi, 1964 (Zagorodnyuk 1990, Rekovets and Nadachowski 1995, Conroy and Cook 2000, Jaarola *et al.* 2004). However, since the 1990s, interspecific crossbreeding experiments, karyological analyses, and molecular studies indicated closer relationships of *Microtus oeconomus* to the eastern Palearctic species of *Alexandromys* Ognev, 1914, although the monophyly of *Alexandromys* was not accepted for a long time (Jaarola *et al.* 2004, Galewski *et al.* 2006, Robovský *et al.* 2008, Bannikova *et al.* 2010, Martínková and Moravec 2012). Recently, Kryštufek and Shenbrot (2022) distinguished three subgenera within the genus *Alexandromys* and classified *A. oeconomus* as a member of the subgenus *Oecomicrotus* Rabeder, 1981.

Previous genetic analyses of *A. oeconomus* based on cytochrome *b* (Brunhoff *et al.* 2003, Bannikova *et al.* 2010) identified four allopatric mitochondrial lineages: Northern European, Central European, Central Asian, and Beringian. According to the above-mentioned authors, geographic distribution of these lineages reflects their isolation during glaciations. However, these studies relied only on modern samples, which may not accurately reflect phylogeographic patterns or colonization routes due to the extinction of old lineages.

Despite the abundant Pleistocene fossils of *Alexandromys* in Eurasia, almost all are linked to the *A. oeconomus* lineage. The oldest remains of *Alexandromys* ex gr. *oeconomus* (Markova 1982), classified as *Alexandromys protoeconomus* (Rekovets, 1994) occur in Russia and Ukraine (Agadzhanyan 1992, Rekovets 1994, Markova 1998) and date to Marine Isotopic Stage (MIS) 21–19, aged approximately 0.9–0.8 Ma (million years ago) (Velichko *et al.* 1983, Markova 2005, Krokhmal' *et al.* 2021, 2023).

Timing of *Alexandromys* lineages divergence is still controversial. Bannikova *et al.* (2010) estimated their separation at *c.* 1.2 Ma, whereas Abramson *et al.* (2021) proposed an earlier split (1.8–2.2 Ma). These studies assumed different evolutionary rates, which also led to varying divergence times for tundra vole lineages. For example, the separation of European and Asian from American lineages was estimated by Brunhoff *et al.* (2003) to 0.29–0.49 Ma, whereas by Bannikova *et al.* (2010) to 0.14–0.24 Ma. These inconsistencies prevent reliable conclusions about climate and environmental impacts on migrations and population changes.

Therefore, the aim of this study is to reconstruct the phylogeny and evolutionary history of *A. oeconomus* using ancient DNA samples. Specifically, we examine population dynamics, migration routes, and extinction, and compare the results of genetic analyses with climate changes during the Late Pleistocene and Holocene. In addition, to the commonly used molecular marker cytochrome

b, we also studied complete mitochondrial genomes of the *A. oeconomus* individuals.

MATERIALS AND METHODS

Sample description

We extracted ancient DNA from the first lower molars (m1) morphologically assigned to *A. oeconomus* (Fig. 1). However, genetic verification was necessary, as some samples were found to be other rodents, e.g. *Chionomys nivalis*. The samples came from 26 localities of the Late Pleistocene and Holocene age (Supporting Information, Table S1). Modern DNA samples were derived from muscle tissues of individuals, which were collected in the field from nine localities (Supporting Information, Table S2). The samples represented various Eurasian regions (Fig. 2).

Radiocarbon dating

Ten samples were selected for dating (see Radiocarbon dating methods in Supporting Information for details). Their collagen was extracted and underwent quality assessment using C/N ratios at the Department of Human Evolution at the Max Planck Institute for Evolutionary Anthropology (MPI-EVA, Leipzig, Germany). Radiocarbon dating was performed in the Laboratory of Ion Beam Physics at ETH-Zurich (Switzerland) using the MIni CArbon DAting System (MICADAS) accelerator mass spectrometer (AMS). The dates were calibrated in Oxcal 4.4 software (Ramsey 2009) using the IntCal 20 curve (Reimer *et al.* 2020) (Table 1).

DNA extraction, sequencing library preparation, and target enrichment

DNA from 148 subfossil samples was extracted and amplified (Supporting Information, Table S3) in a dedicated clean room at the Centre of New Technologies, University of Warsaw (CeNT, UW). Subfossil molars were rinsed with nuclease-free water and crushed in sterile tubes. Total DNA was extracted following the protocol optimized for degraded DNA sequences with negative controls, i.e. without molars, per batch (Dabney *et al.* 2013). Modern DNA from 33 specimens (Supporting Information, Table S4) was extracted using a Syngen Tissue DNA Mini Kit at the Mammal Research Institute of the Polish Academy of Sciences in Białowieża, Poland (Stojak *et al.* 2015), followed by quality checks on a 1% agarose gel and shearing on a Covaris S220 sonicator to a mean length of 200 bp at CeNT.

Genomic DNA was converted into double-stranded dual-indexed libraries following the protocol of Meyer and Kircher (2010) with modifications (Baca *et al.* 2019). The libraries were amplified using AmpliTaq Gold 360 DNA polymerase (Applied Biosystems) and P5 and P7 indexing primers containing a 7-bp long specific index. An index PCR reaction was performed three times for every sample to increase the complexity of the resulting libraries.

Mitochondrial DNA (mtDNA) was enriched via target enrichment according to Horn (2012). The bait used in hybridization was prepared from the mtDNA of five modern vole species including *A. oeconomus*. Mitochondrial DNA was amplified in four overlapping fragments, purified, mixed in equimolar ratios, sonicated to the average fragment length of 200 bp, and modified following Maricic *et al.* (2010). Hybridization (65°C for 22–24 h) included two rounds for ancient DNA (aDNA) and one round for modern DNA. After each hybridization cycle, the library was amplified in a post-capture PCR reaction and purified using magnetic beads. Enriched libraries were quantified using qPCR (Illumina Library Quantification kit, KAPA) and sequenced in a paired-end layout on an Illumina NextSeq550 platform using 150 cycles, MidOutput kits, and a 2 × 75 bp sequencing scheme. Details about the molecular methods of the samples (DNA extraction, sequencing library preparation and target enrichment) are included in Supporting Information.

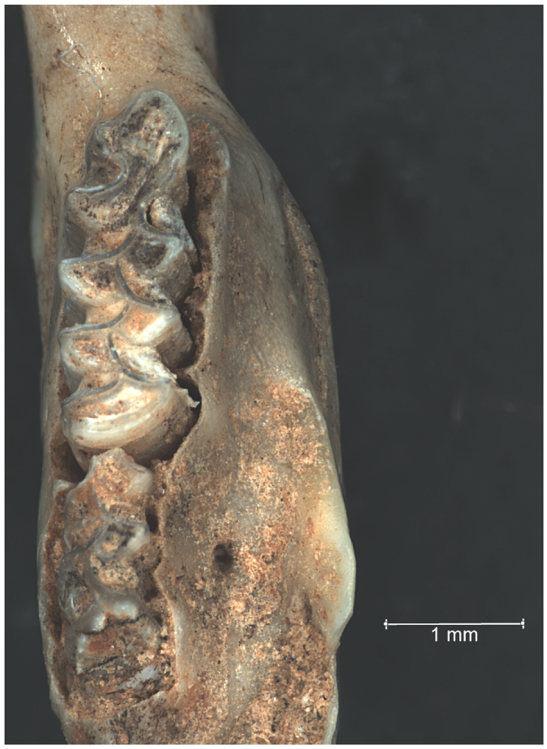

Figure 1. The right mandible with the first (m1), second (m2), and a fragment of the third (m3) molars of fossil *Alexandromys oeconomus* found in layer III of the Obłazowa Cave WE in Poland.

Sequence data processing

Demultiplexing of raw Illumina sequence reads was conducted in bcl2fastq Conversion Software v.2.20 (Illumina) with sample-specific indices. AdapterRemoval v.2 (Schubert *et al.* 2016) removed adapter sequences and low-quality nucleotides as well as collapsed paired-end reads. We mapped reads with the BWA-MEM algorithm in bwa 0.7.17 (Li and Durbin 2010). Initially, the reads were mapped to mtDNA sequence of closely related species, *Alexandromys fortis* (NC_015243), and then to *de novo* constructed more specific references from the high-coverage Eurasian samples of *A. oeconomus*. We visualized alignments in TABLET (Milne *et al.* 2016) and removed PCR duplicates, short reads (< 30 bp), and low-quality reads (MAPQ < 30) using SAMtools. Regions with sequencing coverage lower than 3× were replaced with 'N' to indicate uncertain bases using Bedtools (Quinlan and Hall 2010). The nucleotide variants and consensus sequences (FASTA) were called using BCFtools (Danecek *et al.* 2021). We assessed DNA damage patterns characteristic of ancient DNA with MapDamage v.2 (Ginolhac *et al.* 2011) and visualized sequences in AliView (Larsson 2014).

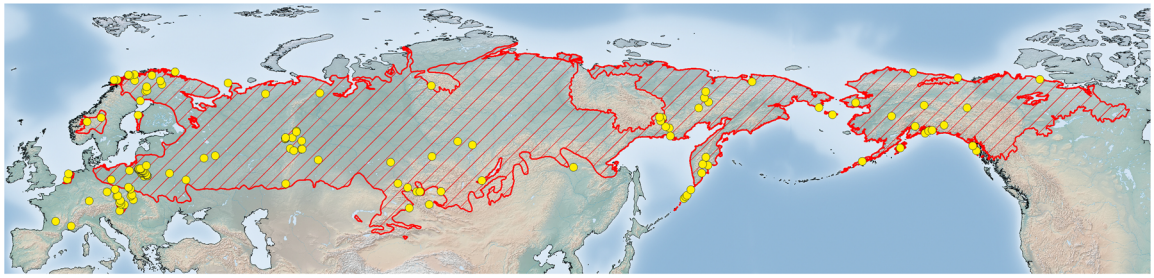

Figure 2. Distribution of the *Alexandromys oeconomus* samples included in this study. The red dashed area reflects the modern range of the tundra vole based on data from the IUCN Red List (www.iucnredlist.org).

Table 1. Radiocarbon-dated samples of *Alexandromys oeconomus*.

AMS lab. code	Lab. ID	Site	C^{14} age BP ± error	Calibrated BP					Element concentration		
				95% confidence interval		μ	σ	Median	C%	N%	C:N
				from	to						
ETH-105991	MI1040	Shelter in Smoleń III	10455 ± 22	12610	12193	12449	134	12483	38.2	13.1	3.4
ETH-105992	MI1088	Perspektywiczna Cave	39180 ± 450	43285	42301	42764	265	42728	43.8	15.4	3.3
ETH-110552	MI1225	Peyrazet	14106 ± 103	17417	16911	17171	133	17174	39.9	13.2	3.5
ETH-110553	MI2190	Obłazowa Cave WE	12567 ± 37	15129	14589	14933	130	14961	41.9	14.6	3.3
ETH-110554	MI2198	Obłazowa Cave WE	12456 ± 88	15031	14202	14628	226	14623	41.3	14.3	3.4
ETH-110555	MI2344	Obłazowa Cave WE	12467 ± 37	14965	14334	14662	168	14644	43.1	15.1	3.3
ETH-110536	MI1037	Shelter in Smoleń III	12418 ± 36	14867	14280	14559	171	14531	41.5	14.1	3.4
ETH-110537	MI2035	Geißenklösterle	29338 ± 154	34308	33453	33921	211	33939	42.5	14.2	3.5
ETH-110538	MI2349	Zamkowa Dolna Cave	12565 ± 36	15125	14590	14930	129	14959	42.0	14.8	3.3
ETH-110539	MI1560	Makhnevskaya 2	11913 ± 35	14004	13606	13772	95	13774	42.5	14.3	3.5

Phylogenetic analyses

We analysed the set (named cytb) including cytochrome *b* sequences and the set (named mtDNA) of 37 concatenated mitochondrial protein and RNA genes as well as noncoding sequences. To the newly obtained sequences, we added those from GenBank. Each set included *Alexandromys fortis* (NC_015243) as an outgroup. Alignments were generated with MAFFT (Katoh and Standley 2013). The final cytb alignment with 1143 bp included 320 unique sequences and mtDNA with 16352 bp contained 181 sequences.

We applied three approaches: maximum likelihood in IQ-TREE (Nguyen *et al.* 2015), Bayesian inference in MrBayes (Ronquist *et al.* 2012), and PhyloBayes (Lartillot and Philippe 2004). All potential data partitions were evaluated to identify the optimal substitution models, with separate partitions defined for each codon position of protein-coding genes, as well as for individual RNA genes and non-coding regions. Details about the phylogenetic analyses are included in the Supporting Information.

In IQ-TREE, we used ModelFinder (Chernomor *et al.* 2016, Kalyaanamoorthy *et al.* 2017) to select the best substitution models (Supporting Information, Tables S6, S7) and a more thorough nearest neighbour interchange (NNI) tree search. Branch support was assessed via the Shimodaira–Hasegawa-like approximate likelihood ratio test (SH-aLRT) with 10000 replicates and the non-parametric bootstrap with 1000 replicates. In MrBayes, we used the partitioned scheme of substitution models from PartitionFinder (Lanfear *et al.* 2012) (Supporting Information, Tables S6, S7) and applied mixed models to select the models from the large parameter space. Two runs using 32 Markov chains were applied for 40 million (for cytb set) or 30 million (for mtDNA set) generations. In PhyloBayes, we applied the CAT-GTR+Γ model and two Markov chains with 100000 generations. A posterior consensus was calculated after the runs converged in these two approaches. Consensus trees from all methods were obtained in IQ-TREE. Alternative tree topologies for the cytb set were evaluated by five available tests in IQ-TREE and Bayes Factor calculated in MrBayes using the stepping-stone method.

Molecular dating

Divergence times of *A. oeconomus* sequences were estimated using BEAST 1.10.4 (Drummond *et al.* 2012) with substitution models proposed by PartitionFinder (Supporting Information, Tables S6, S7). Calibration of the tree relied on the uniform distribution of tip dates from 10 radiocarbon-dated samples and ranged between 95% confidence intervals of the calibrated dates. For samples from well-stratified deposits (Dyrovatyy Kamen, Obłazowa 2, Obłazowa WE, Peyrazet, Rasik series 1–28), we used a uniform distribution between median start and end dates from the OxCal 4.4 trapezium model based on existing radiocarbon dates from these deposits. In the case of samples from Rasik series 29–33, we applied the lognormal distribution with the median of radiocarbon-dated samples 41907.25 and offset based on the median start date from the trapezium model for these series (Supporting Information, Table S8). For other tip dates, we assumed the lognormal distribution with the median 14801.5, i.e. the median of

radiocarbon-dated samples, and 97.5% highest posterior density (HPD) 621000 corresponding to the oldest *A. oeconomus* (Markova and Puzachenko 2018).

Posterior distributions of parameters were estimated over 700 million to 1 billion generations sampled every 1000 steps. Convergence and sampling adequacy were verified using loganalyzer and Tracer v.1.7. All parameters had effective sample size (ESS) exceeding 200. Consensus trees were summarized in TreeAnnotator with a 10% burn-in and assuming common ancestor heights. The final trees were visualized in FigTree 1.4.3. The effective population size was estimated under the best-fit model in Tracer assuming 500 bins.

We tested various tree and clock models, both strict and lognormal relaxed (Supporting Information, Table S9). The best-fitting models were selected according to the marginal likelihood values estimated via path sampling and the stepping stone algorithms (Xie *et al.* 2011, Baele *et al.* 2012) assuming 10 million chain length and 20 steps. Compared models included: coalescent constant size, coalescent Bayesian SkyGrid, coalescent GMRF Skyride with time-aware and uniform smoothing, as well as coalescent Bayesian Skyline piecewise-constant and piecewise-linear (Supporting Information, Table S9). The models were compared using Bayes Factor calculated in BEAST (Supporting Information, Fig. S1).

The results of molecular dating were compared with the $\delta^{18}O$ records from ice cores and benthic foraminifera, commonly used as climate proxies. The $\delta^{18}O$ curve was compiled from: North Greenland Ice Core Project 1 and 2 (NGRIP1 and NGRP2) (Rasmussen *et al.* 2014, Seierstad *et al.* 2014), the Combined Cariaco and Greenland Ice Core Chronology 2005 (GICC05) (Cooper *et al.* 2015) and the benthic curve (Lisiecki and Raymo 2005).

Reconstruction of ancestral geographic distribution

Ancestral geographical distributions of phylogenetic lineages were inferred using BioGeoBEARS, i.e. BioGeography with Bayesian (and likelihood) Evolutionary Analysis with R Scripts, in RASP (Matzke 2013, Yu *et al.* 2015), implemented in R (R Core Team 2022). We tested three biogeographic models: (i) Dispersal-Extinction Cladogenesis (DEC), (ii) DIVALIKE, similar to the Dispersal-Vicariance Analysis (DIVA) model but based on the maximum likelihood method, and (iii) BAYAREALIKE similar to the Bayesian BayArea model but also based on the maximum likelihood method. Each of these models was also considered with the +J version taking into account speciation resulting from the founder effect. The best model was selected based on the second-order Akaike Information Criterion weight (AICc_wt). Analyses were conducted on two chronograms, based on cytochrome *b* sequences and mitochondrial genomes.

RESULTS

Phylogenetic analyses

Phylogenetic relationships between *A. oeconomus* samples were inferred from the molecular marker cytochrome *b* and complete mitochondrial genomes. While the former set had more samples, the latter provided better resolution. Both datasets allowed us to reconstruct the most probable evolution of *A. oeconomus* since the Pleistocene.

Figure 3 shows a simplified consensus of cytochrome *b* trees obtained with three approaches, whereas the full consensus tree is presented in Supporting Information, Fig. S2. The tree identified 12 groups of sequences with shared evolutionary history and/or geographical locality (Figs 3, 4; Supporting Information, Fig. S2). Eleven groups were consistent across all three methods and obtained usually high statistical support. Relationships between them were also statistically significant in most cases. The earliest diverged group A included two ancient samples from Denisova Cave in Central Asia, which clustered together in two Bayesian approaches but branched sequentially in the maximum likelihood tree.

Other sequences created two main lineages. One included groups named from B to D, which occurred only in Asia (Fig. 3; Supporting Information, Fig. S2). Group B contained ancient and recent samples widely distributed from the Urals to Central Asia. Within this cluster was embedded group C comprising recent samples from Northeast Asia. Interestingly, other specimens from Northeast Asia as well as Kamchatka and the north-western part of North America were in group D, which was sister to the assemblage B + C.

North American sequences belonging to group D were not monophyletic but instead formed three distinct clusters, as supported by two or three methods (Supporting Information, Fig. S2). One clade was dominated by 43 American sequences and included one from Northeast Asia. The second clade grouped only two samples from America and 13 from Kamchatka and the Kuril Islands. The third clade had seven specimens from America and six from Northeast Asia.

The second main lineage comprised groups E to L, which represented not only Asia but also Europe (Fig. 3; Supporting Information, Fig. S2). Ancient samples from the Central Urals (group E) were separated first in the phylogenetic trees. MrBayes and IQ-TREE trees demonstrated early divergence of ancient French specimens (group F) followed by two sister lineages: G + H + I + J and K + L but PhyloBayes tree clustered group F with G. The G + H + I + J lineage was geographically diverse. The ancient samples of group G from Central and East Europe were represented by many early diverged branches within this lineage. G evolved into sister groups H and I + J. The former included recent samples from East Europe and Fennoscandia, whereas the latter contained recent samples not only from Fennoscandia (group I) but also ancient and recent specimens from the Urals and recent ones from Northeast Europe (group J). According to the IQ-TREE and MrBayes trees, groups I and J clustered together, whereas the PhyloBayes tree grouped J with H. Neither relationship received strong support. Group K was rich in ancient and recent sequences from Central and Western Europe but also included several recent samples from Fennoscandia assigned to group L.

The modern Netherlands population was geographically separated from others in Europe (Fig. 4). In the phylogenetic tree (Supporting Information, Fig. S2), its samples clustered with fossil specimens from Poland. This pattern may suggest that the population from the Netherlands constitutes a relic lineage persisting from the past.

The clades defined in the cytochrome *b* tree were also indicated in the tree reconstructed from the mitochondrial genomes (Fig. 5; Supporting Information, Fig. S3). However, these two trees

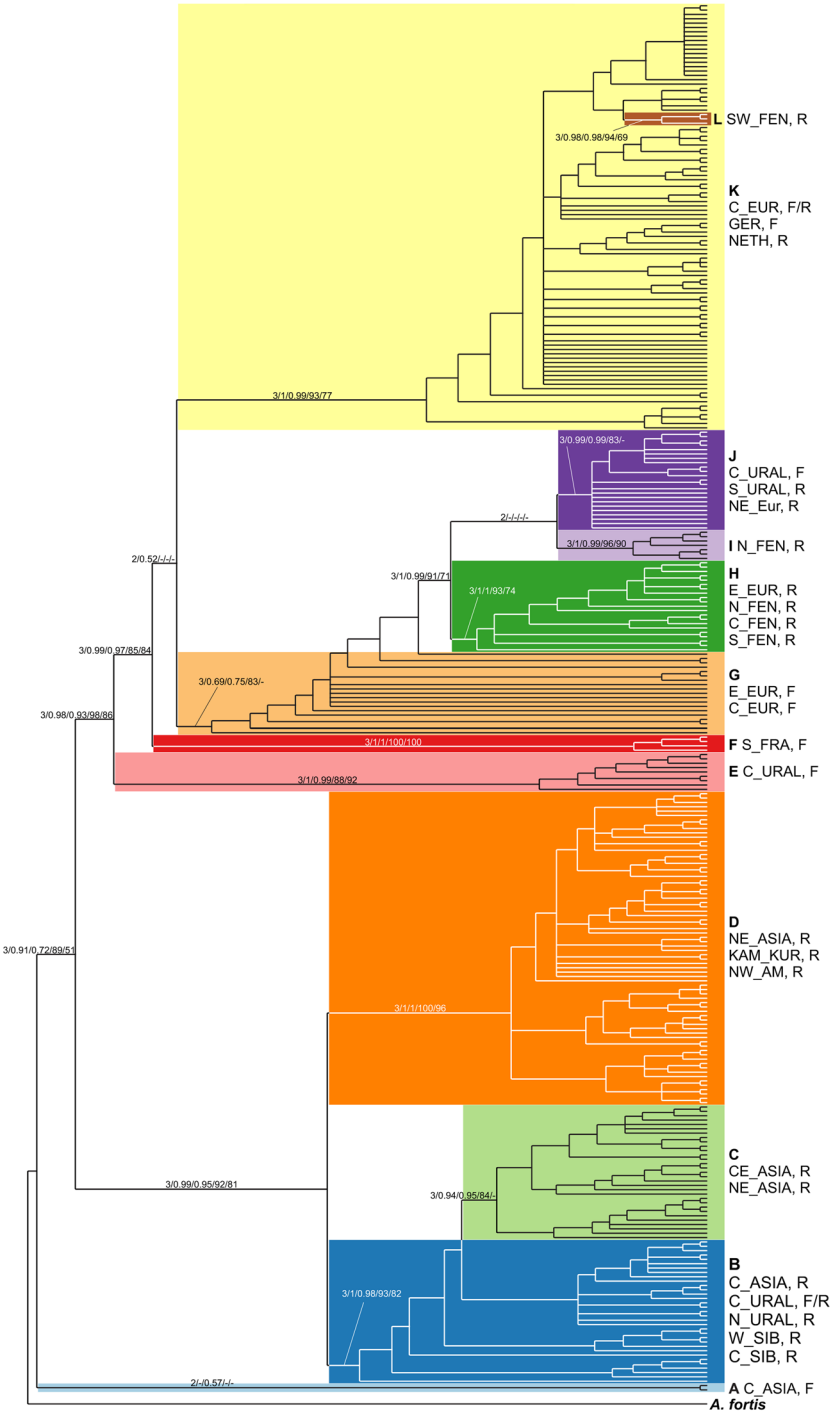

Figure 3. Simplified phylogenetic consensus tree obtained in three programs based on *Alexandromys oeconomus* cytochrome *b* sequences. The values at the nodes in the following order indicate: the number of methods (out of three) that calculated a given taxa (sequence) grouping on the tree, the probabilities calculated in MrBayes and PhyloBayes, as well as the SH-aLRT method, and the bootstrap percentages obtained in IQ-TREE. Posterior probabilities < 0.5 and percentages < 50% are omitted or marked with a dash '-'. The colours indicate distinguished groups marked from A to L. Abbreviations describing the geographical distribution are explained in Supporting Information, Table S5.

differed in the placement of two groups. In the mitogenomic tree, the earliest lineage was B comprising ancient and recent samples from the Urals to Central Asia, rather than group A, which branched later, before group E. Another difference was that group F, containing ancient sequences from France, was sister to group K and did not represent the earliest diverged European lineage. In the mtDNA tree, the first evolved lineage was group G, which included ancient samples from Central and East Europe.

Testing alternative tree topologies

Due to some phylogenetic relationships lacking strong support and differing between the cytochrome *b* and mtDNA trees, we tested

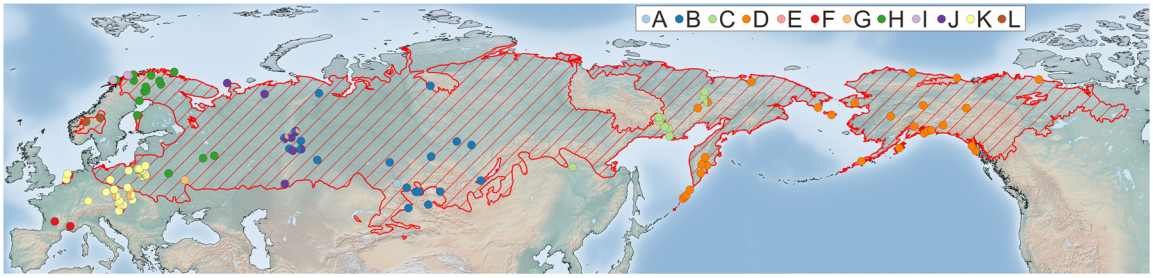

Figure 4. Distribution of *Alexandromys oeconomus* samples assigned to groups distinguished in phylogenetic analyses and marked with colours and letters. The red dashed area reflects the modern occurrence of the tundra vole based on data from the IUCN Red List (www.iucnredlist.org).

these conflicting topologies. In the cytochrome *b* tree, we tested the later divergence of group A, examining its clustering with the clade containing the E-L groups, as shown in the mitogenome-based tree (topology t1 in Fig. 6). The maximum likelihood tests did not reject this possibility, but the Bayesian approach yielded a Bayes Factor of 3.3, surpassing the threshold of 3 (Kass and Raftery 1995) and supported the original topology (topology t0 in Fig. 6). The other topology (t2 in Fig. 6) assuming the sisterhood of group F and K + L in the mtDNA tree was not significantly rejected by any method. We also verified the monophyly of Fennoscandia samples separated by several Eastern European samples in group H (topology t3 in Fig. 6), but it was not significantly rejected either. However, the monophyly of Fennoscandian sequences from group H and the sister group I (topology t4 in Fig. 6) was significantly denied, with Bayes Factor greater than 5, indicating an overwhelming support for the original topology. We also tested if the relationships in the cytochrome *b* tree were significantly worse than those in the mitogenome-based tree (Fig. 7). Three tests showed that the earlier divergence of group A (topology t1 in Fig. 7) in the cytochrome *b* tree, was significantly less likely than the original topology (topology t0 in Fig. 7). However, topology t2, assuming a close relationship between K and G + H + J with F as their sister group as in the cytochrome *b* tree, was significantly rejected by almost all methods in the mitogenome data. Overall, these tests suggest that the topology recovered from the mitogenomic dataset cannot be rejected for the cytochrome *b* dataset.

Molecular dating

Out of 12 tested models, the coalescent GMRF Skyride model with uniform smoothing and the constant clock turned out to be the most appropriate for the data both for the cytb and mtDNA datasets (Supporting Information, Fig. S1), so the final chronograms are presented for this model (Figs 8, 9; see Supporting Information, Figs S4, S5 for the full version). Most nodes associated with the separation of main lineages and groups received high posterior probabilities. The chronogram based on mitogenome sequences matched the same topology as phylogenetic trees computed on these data, whereas the cytochrome *b* chronogram differed only in clustering of groups H and I together with a low support of 0.42, in contrast to phylogenetic methods that joined group I with J (MrBayes and IQ-Tree) or H with J (PhyloBayes).

Supporting Information, Table S10 summarizes the time estimates for tree nodes that corresponded to each other in the two datasets. On average, divergence times were 15.5 ka older in the mitogenome-based chronogram. The largest difference reached *c.* 34 ka for the tree root, whereas the smallest was only 118 years and referred to the common ancestor of group J sequences. Generally, younger divergence times showed smaller differences in age estimates between the datasets. Despite the differences in median values, the ranges of 95% HPD overlapped for the corresponding nodes, indicating consistency in the broader confidence intervals.

Using the molecular dating results, we collected the most probable separation times of the main lineages and groups. The description presented below includes age estimates calculated as medians. Based on cytochrome *b* sequences, the earliest lineage, represented by samples from Denisova Cave in Central Asia from group A, separated around 107 ka (Fig. 8; Supporting Information, Fig. S4) and at approximately 97 ka, there was a split into two main phylogenetic lineages: the Asian-American B-D and the mainly European E-L. Mitogenome dating provided a slightly older divergence time of the earliest lineage B (*c.* 142 ka) and the separation of group A (*c.* 138 ka), i.e. before the Last Eemian Interglacial (Fig. 9; Supporting Information, Fig. S5).

The cytochrome *b* chronogram suggests that group B-D split into D (Northeast Asia and North America) and B + C (other Asian samples) around 70 ka (Fig. 8; Supporting Information, Fig. S4). Group C, containing additional Northeast Asian samples, evolved within group B around 16 ka.

The Uralic lineage E, sister to European lineages (F-L), separated around 108 ka (mtDNA) or 79 ka (cytb) and disappeared around 50 ka (mtDNA) or 32 ka (cytb) (Figs. 8, 9; Supporting Information, Fig. S4, S5). The cytochrome *b* chronogram showed group F (France) as the first European lineage, diverging *c.* 70 ka (Fig. 8; Supporting Information, Fig. S4), with groups G-J splitting from K-L around 62 ka. In contrast, mitogenomes suggest G-J separated first, *c.* 95 ka, with F diverging from K about 89 ka (Fig. 9; Supporting Information, Fig. S5).

Differentiation within group G-J started approximately 27–22 ka and was associated with the separation of subgroups H, I, and J, containing samples from various regions of Fennoscandia, north-eastern Europe, and the Urals (Figs. 8, 9; Supporting Information, Fig. S4, S5). Group G evolved first in the G-J lineage and became extinct around 26–23 ka. However, the F lineage persisted until *c.* 15–14 ka. Group L, containing the other Fennoscandian samples, separated the latest, around 11 ka, coinciding with the Pleistocene–Holocene transition.

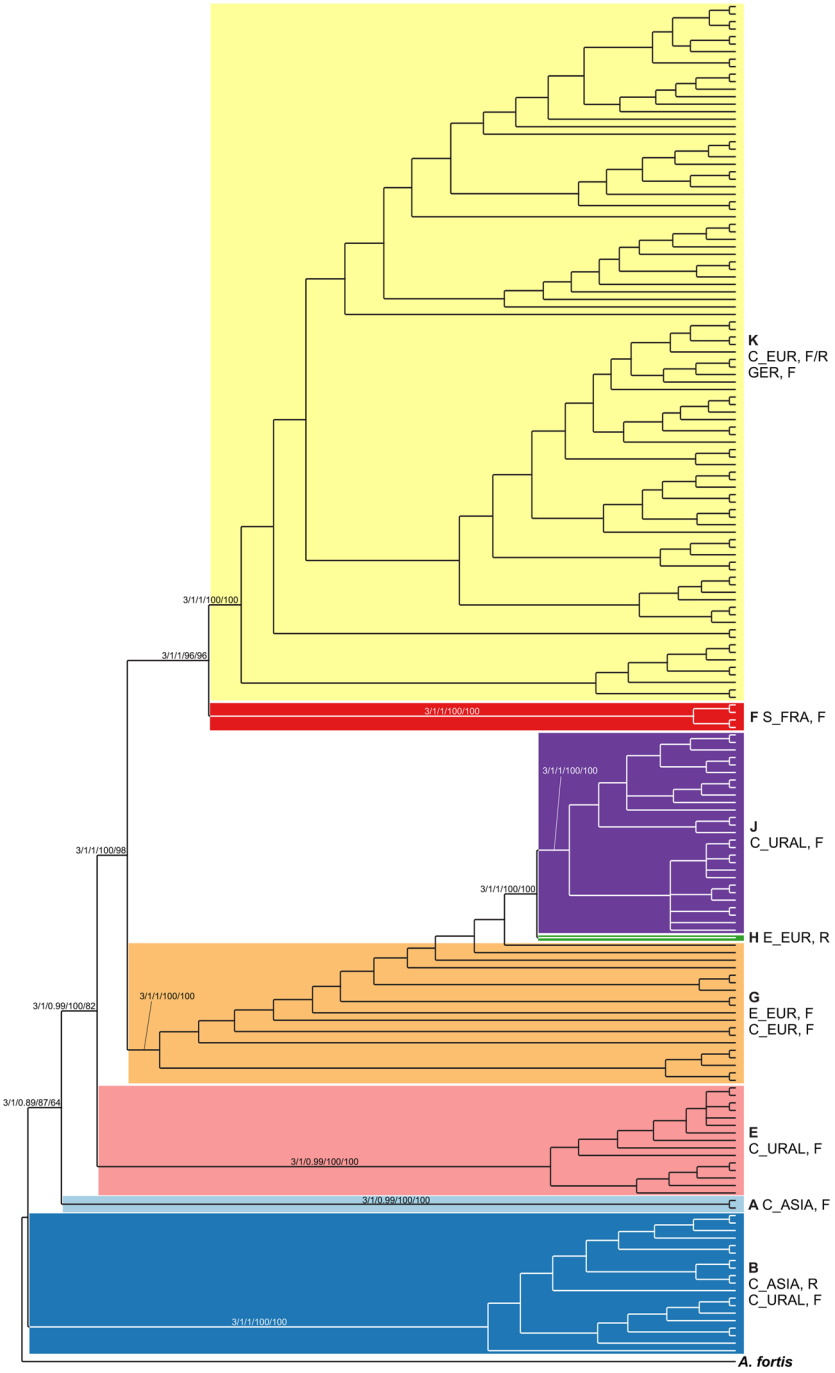

Figure 5. Simplified phylogenetic consensus tree obtained in three programs based on *Alexandromys oeconomus* mitogenome sequences. The values at the nodes in the following order indicate: the number of methods (out of three) that calculated a given taxa (sequence) grouping on the tree, the probabilities calculated in MrBayes and PhyloBayes, as well as the SH-aLRT method, and the bootstrap percentages obtained in IQ-TREE. Posterior probabilities < 0.5 and percentages < 50% are omitted or marked with a dash '-'. The colours indicate distinguished groups marked from A to L. Abbreviations describing the geographical distribution are explained in Supporting Information, Table S5.

In the cytochrome *b* chronogram (Fig. 8; Supporting Information, Fig. S4) and the consensus tree, North American sequences were separated into three clades, which also included Asian specimens. This suggested that at least three haplotypes migrated and diversified in North America. The clade containing most of American sequences diverged around 16 ka and differentiated approximately 14 ka on the American continent. The remaining American clades split from their Asian counterparts around 13 ka and 10 ka.

Reconstructing the geographic distribution of ancestors

After comparing biogeographic models, DEC was the best-fitting for the cytochrome *b* chronogram, with a significantly lower AICc value (Supporting Information, Table S11). For the mitogenome chronogram, the differences between models were smaller, with DIVALIKE emerging as the best model (Supporting Information, Table S11).

After assigning samples to geographic regions (Supporting Information, Fig. S6) and using the best models to infer ancestral

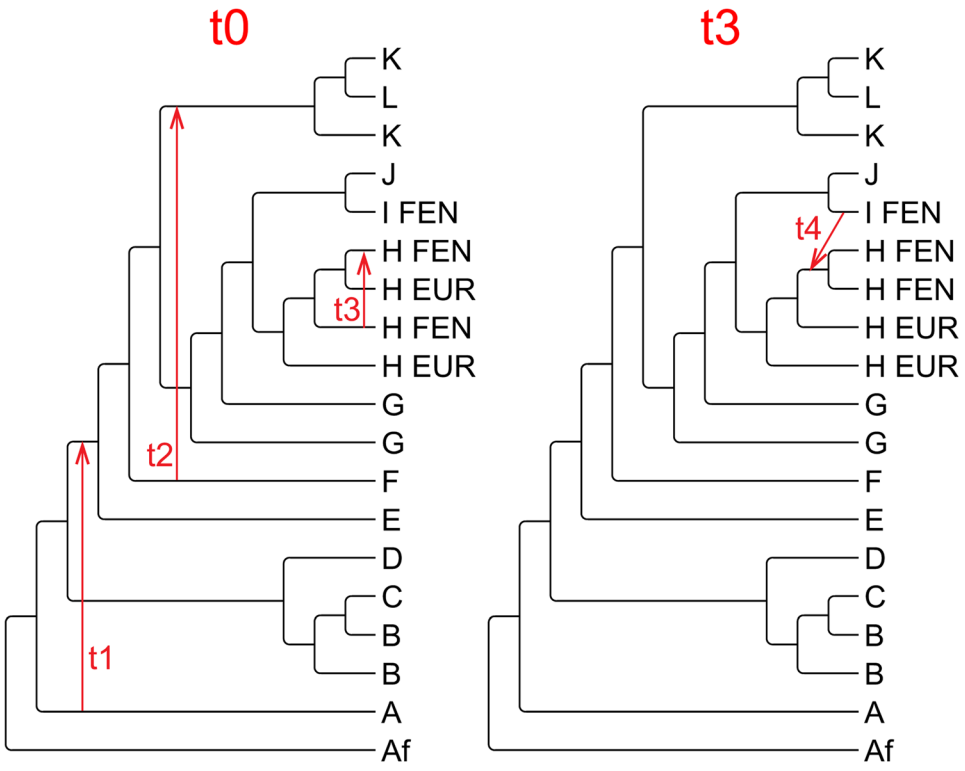

Result of tree topology tests

Tree	bp-RELL	SH	WSH	ELW	AU	BF
t0	0.314	1	0.981	0.324	0.751	0
t1	0.089	0.290	0.218	0.084	0.090	3.30
t2	0.336	0.766	0.706	0.311	0.460	1.79
t3	0.259	0.908	0.849	0.278	0.523	0.67
t4	0.002	0.069	0.035	0.002	0.002	19.4

Figure 6. The simplified best tree for cytochrome *b* sequences (t0) and alternative topologies (t1–t4) assuming other phylogenetic position of selected groups. Results of tests comparing these topologies are shown in the associated table. The table includes: bootstrap proportion using the RELL method (bp-RELL), p-values from the Shimodaira–Hasegawa test (SH), the weighted Shimodaira–Hasegawa test (WSH), the Expected Likelihood Weight test (ELW), and an approximately unbiased test (AU) as well as Bayes Factor (BF) expressed as differences in natural logarithm likelihood units from the best topology (t0). Values smaller than 0.05, and BF > 3 are presented in red font.

distributions, the cytochrome *b* chronogram suggested, with a probability p = 0.63, that the ancestor of tundra voles originated in Central and Western Asia (Supporting Information, Fig. S7), while the mitogenome chronogram indicated Western Asia with p = 0.5 (Supporting Information, Fig. S8). The common ancestor of Asian B, C, and D lineages likely lived in Western Asia (p = 0.74). The B lineage ancestor also resided in Western Asia with probabilities of 0.98 (cytb tree) and 1 (mtDNA tree), before its descendants migrated to Central Asia, where their ancestor had a probability of 0.95 (cytb tree) and 0.57 (mtDNA tree).

Within the B population, the C group emerged and colonized Northeast Asia, with its ancestor in this region with p = 1. The D lineage ancestor independently migrated to Northeast Asia (p = 0.81), from where its descendants populated North America three times, as indicated by the Asian geographic distribution of their ancestors. The common ancestor of the most recently separated Asian lineage and the European E-L groups likely lived in Western Asia, with p = 0.78 (cytb tree) and p = 0.67 (mtDNA tree).

The population from which the European groups emerged also occupied Western Asia, with probabilities of p = 0.81 (cytb tree) and p = 1 (mtDNA tree). The primary region of differentiation for groups G and K could be Central Europe, with p = 0.87 (cytb tree) and p = 1 (mtDNA tree). From there migrations spread to southern France (group F), south-western Fennoscandia (group L), and again to the east. The ancestors of the H-J groups initially inhabited Eastern Europe with a probability of 0.90–1, from where they spread independently twice to Fennoscandia (groups H and I) and the Urals. The analyses indicate that emigration to

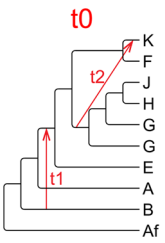

Result of tree topology tests

Tree	bp-RELL	SH	WSH	ELW	AU	BF
t0	0.939	1	0.997	0.926	0.981	0
t1	0.045	0.155	0.085	0.054	0.043	8.3
t2	0.016	0.080	0.041	0.020	0.015	13.7

Figure 7. The simplified best tree for mitochondrial genome sequences (t0) and alternative topologies (t1 and t2) assuming other phylogenetic position of selected groups. Results of tests comparing these topologies are shown in the associated table. The table includes: bootstrap proportion using RELL method (bp-RELL), p-values from the Shimodaira–Hasegawa test (SH), the weighted Shimodaira–Hasegawa test (WSH), the Expected Likelihood Weight test (ELW), and an approximately unbiased test (AU) as well as Bayes Factor (BF) expressed as differences in natural logarithm likelihood units from the best topology (t0). Values smaller than 0.05, and BF > 3 are presented in red font.

north-eastern Europe originated from the Ural region, as the samples from Europe clustered with samples from the Urals.

Fluctuations in effective population size over time

Changes in effective population size over time are presented for the mitogenome data, which contained more sites in the analysis and better reflected population variability than cytochrome *b* data (Fig. 10). These fluctuations were compared with the $\delta^{18}O$ curve, representing global temperature changes. Generally, lower values corresponded to cooling and higher values to warming. Significant decreases and increases in these values could be linked to cold stadials and warm interstadials, respectively.

From the Eemian Interglacial (MIS 5e) through MIS 5a-d, population size showed only slight changes due to limited data for this period. A clear increase began from the Greenland interstadial 22 (GI 22; Andersen *et al.* 2006), continuing until the middle of a cold MIS 4, followed by a decline to a local minimum at GI 14 in MIS 3. From this period, the effective population size rose again to a large local maximum around 35–30 ka, with a brief decline between stadials GS 10 and GS 9. At the end of MIS 3 the population size sharply diminished until the LGM in MIS 2 reached a minimum at the beginning of GS 2.1. As the isotope curve rose, the population size fluctuated, peaking during interstadial 1 (Bølling-Allerød) and decreasing in stadial 1 (Younger Dryas). After reaching a global maximum around 5 ka, it declined and then slightly increased.

Diversity at the population level of groups

The distinguished groups of *A. oeconomus* exhibited varying diversity at the nucleotide level (Fig. 11). The results are similar for cytochrome *b* sequences and mitogenomes. The greatest variability was shown by group B, containing samples from Asia, and group F, represented by extinct samples from southern France. Taking into account cytochrome *b* sequences, the least diverse were groups I (samples from northern Fennoscandia), J (samples from the Urals and north-eastern Europe), and L (samples from south-western Fennoscandia), as well as group A (samples from Denisova Cave). Groups D (sequences from north-eastern Asia and North America) and H (sequences from various areas of Fennoscandia and eastern Europe) also demonstrated relatively high values of diversity.

We conducted Fu and Tajima neutrality tests to assess if subpopulations followed the neutral mutation theory and were in equilibrium with genetic drift. The Fu test for cytochrome *b* data showed significant deviations with negative values for groups B, C, D, G, H, I, J, and K. Group D (-103.2) had the highest negative values, followed by C (-33.6). In contrast, the Tajima test was more conservative, with significant deviations from the expected values in groups D (-2.2), J (-1.9), and K (-2.1) (Supporting Information, Table S12). Analyses of mitogenome data provided similar results. The Fu and Tajima tests exhibited significantly low values for groups J and K, whereas the Fu test indicated significant negative deviations for group G. The lowest values were shown by group K with Fu's Fs = -33.7 and group J with Tajima's D = -2.2. Group F showed positive values in both tests (Supporting Information, Table S13).

DISCUSSION

Evolution of Alexandromys oeconomus populations in time and space

Phylogenetic analyses, based on three methods on the popular marker cytochrome *b* and complete mitochondrial genome sequences, allowed the distinction of 12 main groups of *A. oeconomus* and the reconstruction of their relationships. While cytochrome *b*-based data included many more sequences with greater geographic diversity, the mitogenomic data provided better-resolved phylogenies. Moreover, molecular dating analyses revealed divergence times for individual groups, which were compared with $\delta^{18}O$ records, commonly used as climate proxies.

Our results are generally consistent with other authors (Brunhoff *et al.* 2003, Bannikova *et al.* 2010), who identified four main allopatric phylogenetic lineages in the tundra vole. However, thanks to aDNA, we have distinguished additional groups, highlighting greater past variability in the species and reconstructed the migration routes of *A. oeconomus* populations (Fig. 12). Generally, the analysed sequences can be divided into two large groups, including Asian-American and European samples. Their ancestor most likely lived in the areas of Central and Western Asia. However, it cannot be excluded that the ancestor of the tundra vole may have been a large, mobile population, like contemporary related species, and could have inhabited vast areas of Asia (García-Rodríguez *et al.* 2024).

The earliest separated groups A and B evolved across large areas of Asia from the Urals to the central part of Siberia. The separation of these lineages from other groups occurred at the end of the penultimate glacial period (MIS 6), *c.* 142–138 ka, based on the mitogenomic data. The A lineage became extinct earlier than B, which remained the only one group in Central Asia. This extinction may have been linked to Eemian warming and the expansion of forests, which were unfavourable conditions for the studied species. However, given the small number of samples for the A lineage, the details about their extinction remains speculative.

The common ancestor for the European F–L lineages diverged from the Uralic group E during a relatively warm period at the end of MIS 5e and the beginning of MIS 5a-d, around 108 ka. After migrating west, the tundra vole spread across Europe and

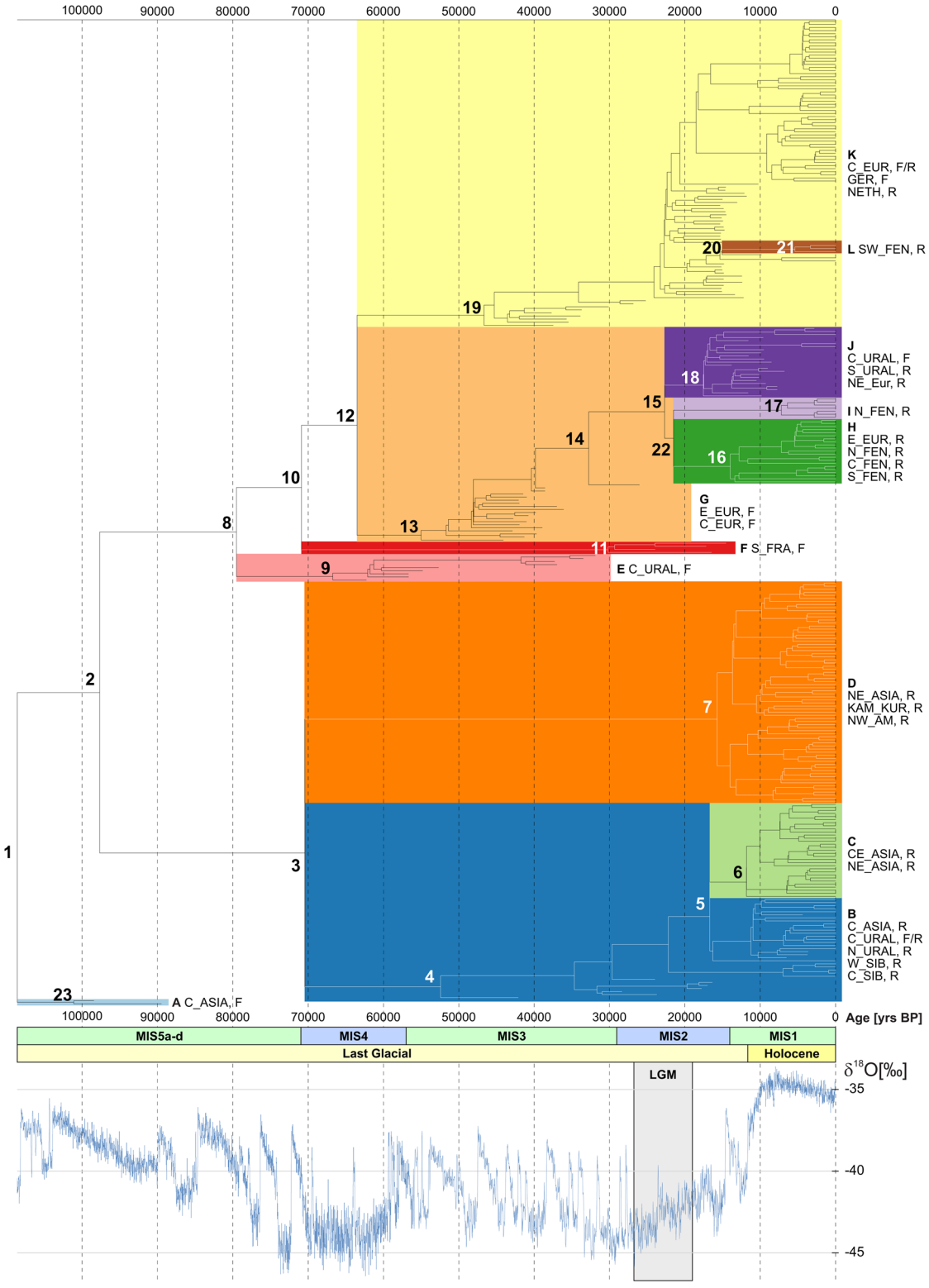

Figure 8. Chronogram obtained for the cytochrome *b* sequences of *Alexandromys oeconomus*. The colours indicate distinguished groups marked from A to L. Abbreviations describing the geographical distribution are explained in Supporting Information, Table S5. Lower part of figure shows a range of different periods and epochs, as well as the $\delta^{18}O$ curve. The numbers on the selected nodes correspond to those given in Supporting Information, Table S10. MIS—Marine Isotope Stage; LGM—Last Glacial Maximum.

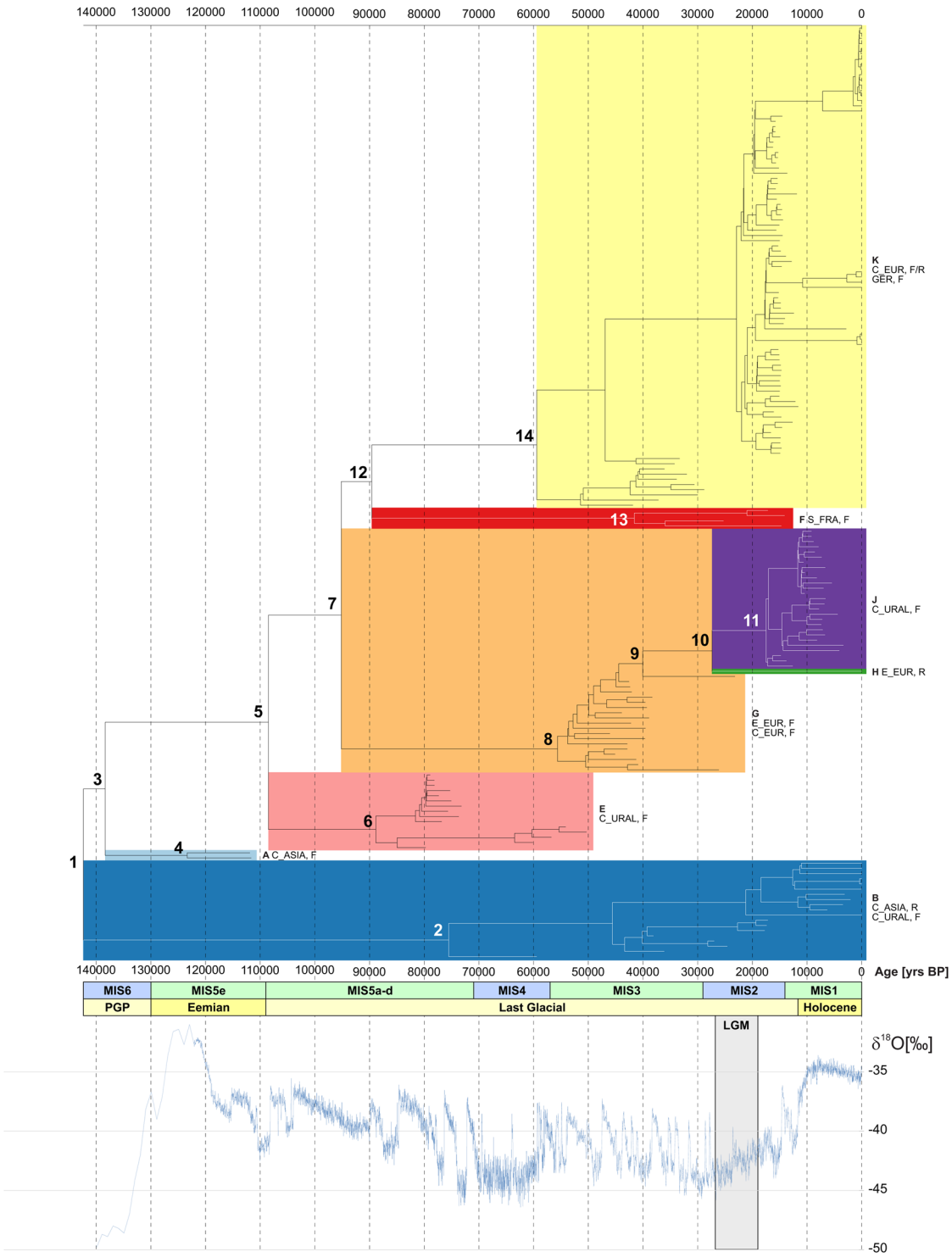

Figure 9. Chronogram obtained for the mitogenome sequences of *Alexandromys oeconomus*. The colours indicate distinguished groups marked by A, B, E–H, J and K. Abbreviations describing the geographical distribution are explained in Supporting Information, Table S5. Lower part of figure shows a range of different periods and epochs, as well as the $\delta^{18}O$ curve. The numbers on the selected nodes correspond to those given in Supporting Information, Table S10. MIS—Marine Isotope Stage; LGM—Last Glacial Maximum.

diversified to individual lineages. From Central Europe, early migrations took place to south-western Europe and later to Northern and Eastern Europe, reaching the Urals (Fig. 12). MIS 5a-d was also the period when, at approximately 95–89 ka, new European groups (F, G-J, K-L) separated and differentiated.

A similar pattern of the mtDNA lineages was observed in European (*Stenocranius anglicus*) and Asian (*S. gregalis*) narrow-headed voles (Baca *et al.* 2023a), the common vole *Microtus arvalis* (98–83 ka) (Baca *et al.*, 2023b), and the collared lemming *Dicrostonyx torquatus* (109–92 ka) (Palkopoulou *et al.* 2016, Lord *et al.* 2022).

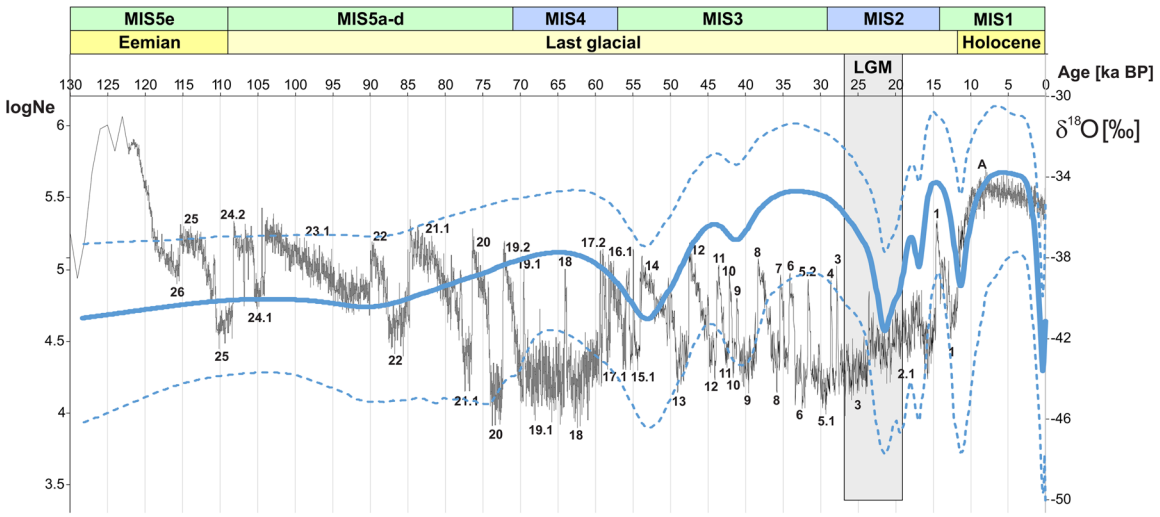

Figure 10. Effective population size (Ne) obtained for the chronogram of mitochondrial genomes compared to the $\delta^{18}O$ curve. The range of different time periods is shown at the top of the figure. MIS—Marine Isotope Stage; LGM—Last Glacial Maximum. The numbers above and below the isotope curve correspond to selected Greenland stages (below) and interstadials (above). Dashed lines correspond to 95% HPD.

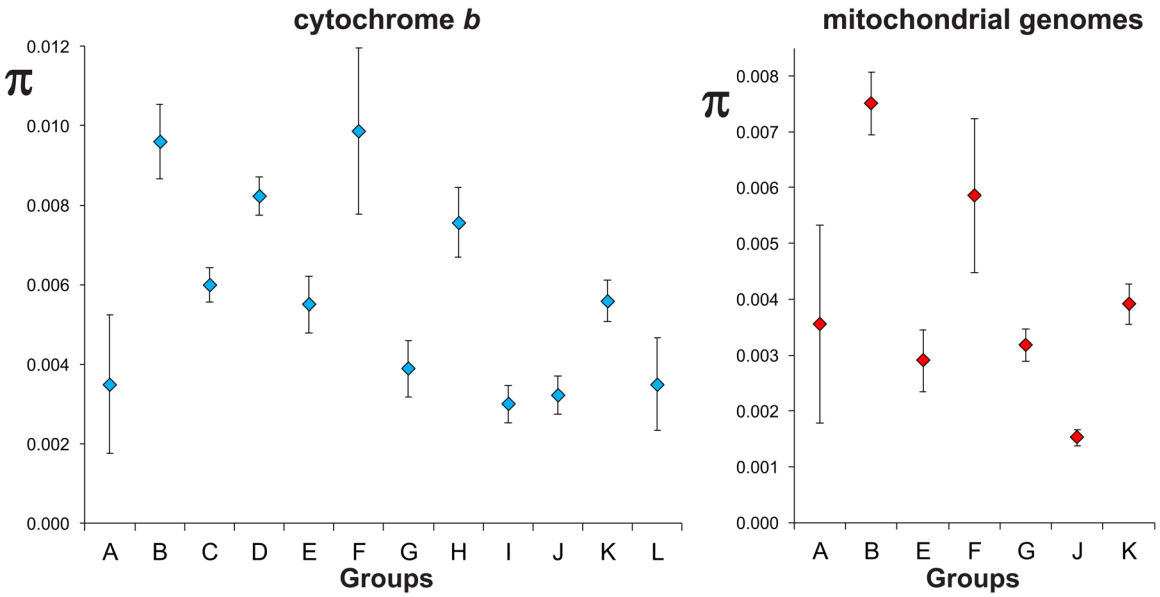

Figure 11. Diversity at the nucleotide level (π) in the distinguished groups of *Alexandromys oeconomus* for two datasets. The diamonds indicate the mean value and the whiskers mark the standard deviation.

This may be related to the Brørup Interstadial (104–88 ka) marked by dense forests (Helmens 2014), which were unfavourable for rodents adapted to open steppe habitats and could have led to the fragmentation of their populations and the emergence of new lineages.

Group D was more expansive. It separated approximately 70 ka from Central Asian groups B-C, settled in north-eastern Asia and later migrated to North America (Fig. 12). In the cold period of MIS 4, no major groups formed, and at the beginning of MIS 3, at approximately 50 ka according to mitogenome data, the Ural E group disappeared. During the relatively warmer MIS 3, approximately 40–33 ka, the ancestor of the H-J groups separated from the Central and Eastern European group G. The ancestral population H-J migrated after 25 ka into the Urals and north-eastern Europe (J) and Fennoscandia (H and I). The initial north-eastern European population most likely lived near the Urals, and the settlement of the Fennoscandian Peninsula took place from Eastern Europe via the Finnish-Karelian Massif. The relationships between H, I, and J remain unclear, although most data (two methods in phylogenetic analyses and one chronogram) indicate that groups I and J are more closely related, with H being a sister group. Nevertheless, Fennoscandian sequences from groups H and I are not monophyletic because they are separated by sequences from Eastern Europe. Thus, we can assume that H and I inhabited Fennoscandia independently. A similar pattern of colonization was observed for other rodents, such as *Microtus agrestis* and *Clethrionomys glareolus* (Herman *et al.* 2014, Marková *et al.* 2020).

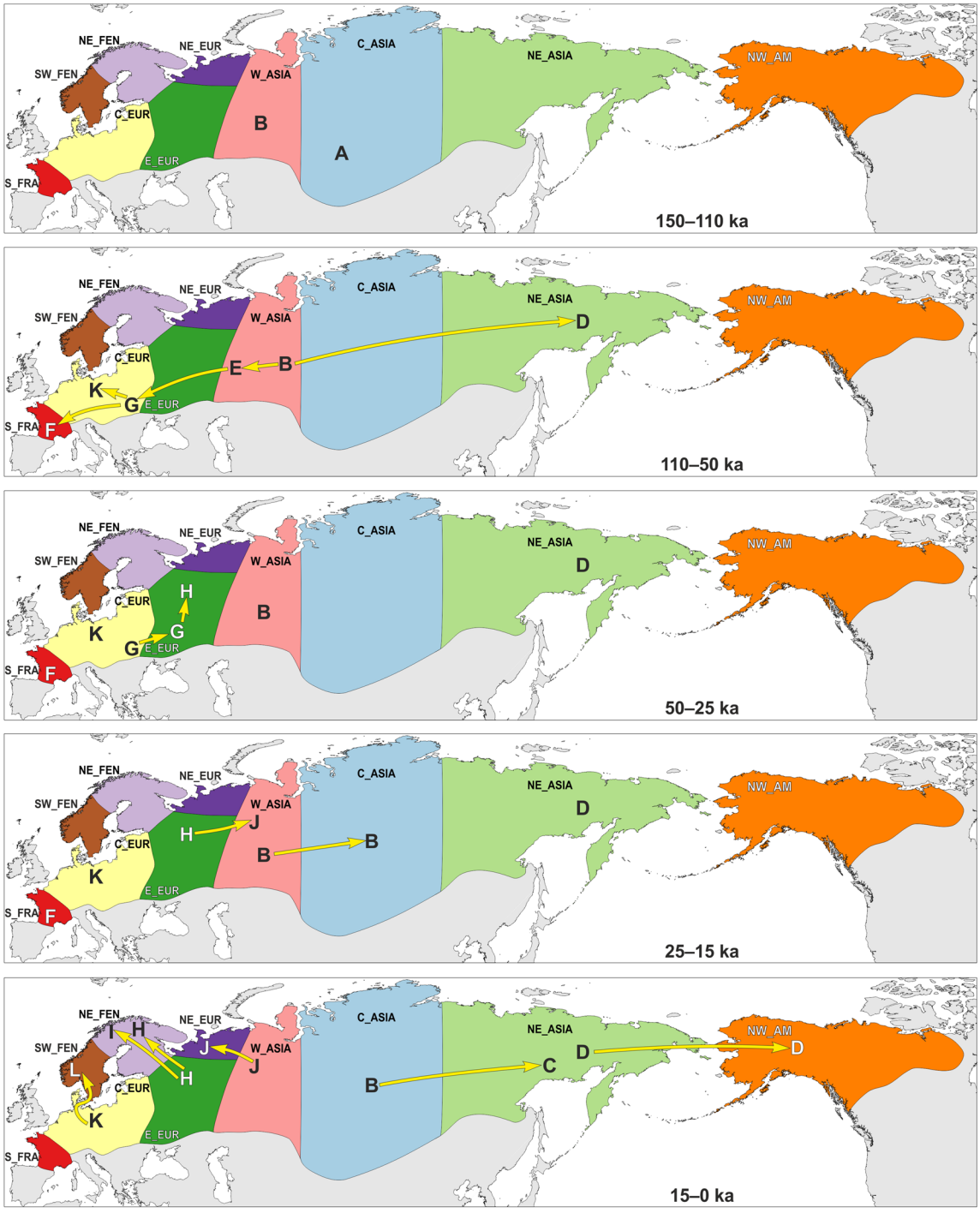

Figure 12. Probable phylogeographic relationships and potential migration directions of distinguished groups of *Alexandromys oeconomus* shown in selected periods. The names of the groups correspond to the designations on the presented phylogenetic trees and chronograms.

Most changes in the mtDNA lineages of the narrow-headed vole, common vole, and lemmings also occurred at the end of MIS 3 between 45 and 30 ka (GS 12 to GS 5.1) (Palkopoulou *et al.* 2016, Lord *et al.* 2022, Baca *et al.* 2023a, Lord *et al.* 2025). For all these rodent species, the time of greatest diversification coincides with the Hengelo-Charbon interstadials (43–41 ka) and Denekamp-Grand Bois (36–33 ka), i.e. brief warmings with the appearance of forests (Helmens 2014). During this time, at the end of MIS 3, between 40 and 26 ka, extinctions or replacements of megafauna genetic lineages occurred (Cooper *et al.* 2015).

During the very cold Last Glacial Maximum (LGM), approximately 26–23 ka, the last representatives of the early lineages of the Central and Eastern European G group became extinct, and its descendants in the H-J groups survived. Group K was the sole lineage in Central Europe. At the end or after the LGM, i.e. 16 ka, a second group called C diverged in Central Asia within B, and like D, independently emigrated to north-eastern Asia (Fig. 12).

During the LGM, when the climate was harsh, but stable compared to the end of MIS 3, tundra and steppe-tundra environments spread over most of Europe and Western Asia. Two turnovers of mtDNA lineages were also recorded in collared lemming populations, when Eurasian groups became extinct and new ones appeared rapidly in the area, *c.* 22–20 ka (Palkopoulou *et al.* 2016). Baca *et al.* (2023a) estimated such population replacement of the narrow-headed vole, *Stenocranius gregalis* from the northern and central Urals at approximately 24–23 ka. This suggests that short-term environmental changes may have affected much of the Eurasian steppe-tundra biome during the LGM.

After the LGM, the tundra vole population expanded from isolated refugia in Central and Eastern Europe across a wider area in these territories and also migrated to Northern Europe (Fig. 12). Another migration occurred also from Central to north-eastern Asia and next to North America.

Reconstruction of the ancestral distribution of American lineages indicates that this continent was settled at least three times from north-eastern Asia. About 15 ka, the main clade of North American populations separated and migrated to this continent before 11.5 ka. These results are consistent with the emergence of a land bridge across the Bering Strait connecting Asia with North America between 30 and 11 ka, during the climate cooling and the accumulation of large masses of water in the ice sheets (Hu *et al.* 2010). It is estimated that the lowest sea level and the widest bridge existed approximately 25–15 ka. The geographic distribution of specimens from this group around the Bering Strait follows the traditional boundaries of the Beringian refugium including Eastern Siberia, Alaska, and north-western Canada. The same pattern has been observed in other species, including the Nearctic lemming (*Lemmus trimucronatus*) (Fedorov *et al.* 1999).

Group F, represented by specimens from southern France, persisted for a relatively long time, which agrees with fossil records of *A. oeconomus* from this region dated to at least MIS 4 (Discamps and Royer 2017), Representatives of this group most likely reached the north of Spain, where the remains of *A. oeconomus* were also found (Cuenca-Bescós *et al.* 2009, Fernández-García *et al.* 2016, Laplana *et al.* 2016, García-Morato *et al.* 2024). Our estimations suggest that group F became extinct around 15–14 ka but it could survive longer, into the Bølling-Allerød Interstadial and possibly until the Younger-Dryas cooling event, according to fossil findings (Royer *et al.* 2016, 2021). The continuous presence of the *A. oeconomus* lineage in south-western Europe parallels the persistence of the *Stenocranius gregalis* lineage during the same period and in the same region (Baca *et al.* 2023a). The population from the Netherlands is currently geographically isolated from other populations and likely represents a relic surviving lineage that diverged from an extinct Central European population around 15.5 ka.

Around 11 ka, during MIS 1 warming, the third colonization of Fennoscandia from Central Europe took place by group L, which evolved within the European K group (Fig. 12). This migration likely occurred via land bridges across the area of the Jutland Peninsula, which existed between Sweden and Denmark 11.2–8.2 ka (Björck 1995, 1996). Today, southern Sweden is separated from continental Europe by the Öresund Strait, although fossil data from Denmark and Sweden indicate that *A. oeconomus* migrated along this route at the end of the Pleistocene (Liljegren 1975), which is additionally confirmed by the results of our analyses.

Previous studies based on modern sequences suggested that the main phylogeographic structure of the modern tundra vole was formed before the last glaciation (Brunhoff *et al.* 2003). In contrast, our studies indicate that only the Asian–European split occurred at that time, whereas most diversification took place during the last glacial. While earlier works proposed colonization of Northern Europe from Central European refugia, our results also support two additional migrations into Fennoscandia from Eastern Europe.

Brunhoff *et al.* (2003) and Iwasa *et al.* (2009) investigating cytochrome *b* noticed a high similarity between specimens from Alaska and north-eastern Russia, suggesting a recent colonization of North America from a relatively homogeneous ancestral population during the last Wisconsin ice age (Rausch 1963). Our findings, however, point to at least three, later migration waves into North America.

The rate of evolution and population diversity of *Alexandromys oeconomus*

We observed fluctuations in the effective population size (N_e) of the tundra vole over time not always aligning in the same way as changes in the oxygen isotope curve. It should be taken into account that changes in N_e could have occurred with a delay relative to the isotope curve variations and environmental changes in different regions may not have responded directly to global climate change due to the high resilience of ecosystems (Holling 1973). However, certain trends can be observed. Generally, the increase in the effective population size was associated with climate warming, and its decrease with cooling, with the greatest reduction occurring during the LGM. Short-term cooling (stadials) and warming (interstadials) had less impact than longer periods on the tundra vole population, though intense changes may have been more influential than temperature extremes.

It should be also considered that the appearance or decline of certain types of environments can be more significant in the differentiation of *A. oeconomus* than only changes in climatic parameters. During warming periods, dense forest clusters of the temperate zone may have appeared, dividing vole populations into smaller ones, preferring open steppe-tundra areas. This could have led to greater genetic diversity due to the isolation of the populations. In turn, excessive warmth or forest cover could reduce suitable habitats, limiting population size. Similarly, extreme climate cooling, e.g. in the LGM, made the conditions too restrictive, which also limited the population size.

Studies of rodents from the stadial 2 (GS-2) to interstadial 1 (GI-1) transition at the end of the last glacial showed that transformations in fauna and environment began over 2 ka earlier and more clearly than the global warming around 14.7 ka (Lemanik *et al.* 2020). This suggests that the climate shift may have occurred in Central Europe (or even across a larger area of this continent) before changes in the $\delta^{18}O$ recorded in the Greenland glacier at the GS-2a/GI-1e boundary. It is also possible that subsequent changes in fauna were not caused by temperature oscillations, but changes in other climatic parameters, such as precipitation and humidity.

Nucleotide sequence analysis revealed that populations with broader geographic ranges and longer evolutionary histories tend to exhibit higher genetic diversity. This applies especially to group B with both a long evolutionary history and wide distribution from the Urals to Central Asia as well as group H, which spread across Fennoscandia and Eastern Europe and group D migrating to Northeast Asia and North America. Additionally, low and significant values in two tests for group D suggest that it recently and rapidly spread across Northeast Asia and reached North America, diverging after the LGM, though it split from other Asian lineages around 70 ka. Fossil samples from southern France (group F) also show a high variability, suggesting a larger historical range in western Europe.

Conversely, groups with the lowest variability, e.g. I and L in Fennoscandia, and J in north-eastern Europe to the Urals, evolved more recently after the LGM in the newly settled areas, likely from small, rapidly expanding populations. The rapid post-LGM expansion from small populations or a bottleneck event that reduced genetic diversity is supported by two neutrality tests for groups J and K. For group J, this likely relates to the migration into north-eastern Europe and the Urals, whereas for group K, it reflects recent spread across currently occupied areas of Central and Western Europe. These findings align with estimated divergence times for both groups.

However, the results should be interpreted cautiously, as classical population genetics parameters may be biased due to heterochrony in the datasets (Depaulis *et al.* 2009). Since the samples within each group represent a narrow period, this effect is likely minimal.

The influence of datasets on the estimation of divergence times

Testing different models of evolution showed that the studied sequences most likely evolved with a constant substitution rate, possibly due to the relatively recent evolutionary timeframe of just over 100 ka. Smaller variability of estimated times when considering longer sequences, i.e. entire mitochondrial genomes, rather than a shorter marker cytochrome *b* are most likely due to the lower variance and higher accuracy of model parameter estimation compared to the shorter sequence with fewer sites in the sequence alignment.

Bannikova *et al.* (2010) estimated the divergence time of European and Asian lineages at 190 ka, whereas both the division of the European population into Russian and Western European lineages as well as the split of the Asian lineage into Siberian and Beringian lineages occurred around 110 ka. These dates were inferred based on cytochrome *b* sequences from a multi-species *Microtus* tree, and the clock calibration assumed radiation of the main *Microtus* lineages at 2.2 Ma. Our estimates were later: 142 ka, 95 ka, and 70 ka, respectively. The earlier overestimations may result from reliance only on modern sequences, rough calibration assumptions, and variability in substitution rates across multiple species.

Even earlier times were obtained by Brunhoff *et al.* (2003) using simple calculations based on the rate of substitutions in cytochrome *b*. According to them, the northern European group separated from the Central Asian group 490–290 ka, and the separation of two European groups (northern and central) occurred 330–200 ka, whereas the Central Asia and Beringia groups diverged 350–210 ka. All these estimates are much older than the separation of even the main European and Asian groups calculated based on our analyses and Bannikova *et al.* (2010). Therefore, it seems unlikely in the light of our results that voles could have entered North America earlier and not diversified on both sides of the strait due to migrations that would allow for population mixing (Brunhoff *et al.* 2003).

ACKNOWLEDGEMENTS

We are very grateful for Dr Mohamed Alsaaraf from the University of Warsaw and Dr Karol Zub from the Mammal Research Institute, Polish Academy of Sciences in Białowieża for providing samples for the analyses. The authors thank Mathieu Langlais and Véronique Laroulandie for providing access to the Peyrazet specimens.

AUTHOR CONTRIBUTIONS

A.Ż., D.P.: conducted the research and investigation process, specifically performing the experiments and data collection; wrote the original draft; P.M.: planned and performed the bioinformatic, phylogenetic, and biogeographic analyses; wrote the original draft and the final manuscript; M.B.: inspected the research activity, planning, and execution; reviewed and edited the manuscript; H.F.: conducted the collagen extraction; reviewed and edited the manuscript; A.L., M.K., J.S., K.S., T.F., I.H., A.K.A., N.V.S., S.E.R., N.C., E.D., A.R., S.P., I.B., L.R., C.B., G.H.: provided study materials; identified species based on morphology; reviewed and edited the manuscript; A.N.: formulated the research aims; provided study materials; identified species based on morphology; reviewed and edited the manuscript.

SUPPLEMENTARY DATA

Supplementary data is available at *Zoological Journal of the Linnean Society* online.

CONFLICT OF INTEREST

The authors declare no conflict of interest.

FUNDING

This work was supported by the National Science Centre Poland (Narodowe Centrum Nauki, Polska) Grant Nos 2017/25/B/NZ8/02005 and 2020/37/N/NZ8/02433 as well as the Interdisciplinary Environmental Doctoral Studies program in the field of Biotechnology and Nanotechnology BioTechNan in the framework of the National Leading Scientific Center (KNOW) at the University of Wrocław. S. E. Rhodes was supported by ICArEHB – Interdisciplinary Center for Archaeology and Evolution of Human Behaviour, funded by the Portuguese Foundation for Science and Technology (FCT) under program UID/04211/2025. The excavations were partially funded by the project RPO WSL Olsztyn Castle – Increasing the attractiveness of Olsztyn Castle through necessary conservation and restoration works, implemented under the Regional Operational Programme of the Silesian Voivodeship for 2014–2020, Priority Axis 5.3: Cultural Heritage, and co-financed by the European Regional

Development Fund. Some computations were carried out at the Wrocław Centre for Networking and Supercomputing, Poland, under Grant No. 307 obtained by P. Mackiewicz.

DATA AVAILABILITY

All data underlying this article are available in the article and in its online Supporting Information. The data underlying this article are also available in the GenBank Database at https://www.ncbi.nlm.nih.gov/ and the European Nucleotide Archive (ENA) at https://www.ebi.ac.uk/ena/browser/home under accession numbers listed in Supporting Information, Tables S3 and S4.

REFERENCES

Abramson NI, Bodrov SY, Bondareva OV *et al.* A mitochondrial genome phylogeny of voles and lemmings (Rodentia: Arvicolinae): evolutionary and taxonomic implications. *PLoS One* 2021;**16**:e0248198.

Agadzhanyan AK. *The Stages of Pleistocene Small Mammal Development in the Central Russian Plain. Staratigraphy and Palaeoenvironment of the Quaternary of Eastern Europe*. Moscow: Institute of Geography RAN Press, 1992. [in Russian].

Andersen KK, Svensson A, Johnsen SJ *et al.* The Greenland Ice Core Chronology 2005, 15–42ka. Part 1: constructing the time scale. *Quaternary Science Reviews* 2006;**25**:3246–57.

Baca M, Nadachowski A, Lipecki G *et al.* Impact of climatic changes in the Late Pleistocene on migrations and extinctions of mammals in Europe: four case studies. *Geological Quarterly* 2017;**61**:291–304.

Baca M, Popović D, Agadzhanyan AK *et al.* Ancient DNA of narrow-headed vole reveal common features of the Late Pleistocene population dynamics in cold-adapted small mammals. *Proceedings of the Royal Society B: Biological Sciences* 2023a;**290**:20222238.

Baca M, Popović D, Baca K *et al.* Diverse responses of common vole (*Microtus arvalis*) populations to Late Glacial and Early Holocene climate changes—evidence from ancient DNA. *Quaternary Science Reviews* 2020;**233**:106239.

Baca M, Popovic D, Lemanik A *et al.* Highly divergent lineage of narrow-headed vole from the Late Pleistocene Europe. *Scientific Reports* 2019;**9**:17799.

Baca M, Popović D, Lemanik A *et al.* Ancient DNA reveals interstadials as a driver of common vole population dynamics during the last glacial period. *Journal of Biogeography* 2023b;**50**:183–96.

Baele G, Lemey P, Bedford T *et al.* Improving the accuracy of demographic and molecular clock model comparison while accommodating phylogenetic uncertainty. *Molecular Biology and Evolution* 2012;**29**:2157–67.

Bannikova AA, Lebedev VS, Lissovsky AA *et al.* Molecular phylogeny and evolution of the Asian lineage of vole genus *Microtus* (Rodentia: Arvicolinae) inferred from mitochondrial cytochrome *b* sequence. *Biological Journal of the Linnean Society* 2010;**99**:595–613.

Banuls-Cardona S, Lopez-Garcia JM, Blain HA *et al.* The end of the Last Glacial Maximum in the Iberian Peninsula characterized by the small-mammal assemblages. *Journal of Iberian Geology* 2014;**40**:19–27.

Berto C, Rubinato G. The Upper Pleistocene mammal record from Caverna degli Orsi (San Dorligo della Valle—Dolina, Trieste, Italy): a faunal complex between eastern and western Europe. *Quaternary International* 2013;**284**:7–14.

Björck S. A review of the history of the Baltic Sea, 13.0-8.0 ka BP. *Quaternary International* 1995;**27**:19–40.

Björck S. Late Weichselian/Early Preboreal development of the Öresund Strait; a key area for northerly mammal immigration. *Acta Archaeologica Lundensia* 1996;**8**:123–34.

Blois JL, McGuire JL, Hadly EA. Small mammal diversity loss in response to Late-Pleistocene climatic change. *Nature* 2010;**465**:771–4.

Brace S, Palkopoulou E, Dalén L *et al.* Serial population extinctions in a small mammal indicate Late Pleistocene ecosystem instability. *Proceedings of the National Academy of Sciences of the United States of America* 2012;**109**:20532–6. I.

Brunhoff C, Galbreath KE, Fedorov VB *et al.* Holarctic phylogeography of the root vole (*Microtus oeconomus*): implications for Late Quaternary biogeography of high latitudes. *Molecular Ecology* 2003;**12**:957–68.

Campos PF, Willerslev E, Sher A *et al.* Ancient DNA analyses exclude humans as the driving force behind Late Pleistocene musk ox (*Ovibos moschatus*) population dynamics. *Proceedings of the National Academy of Sciences of the United States of America* 2010;**107**:5675–80.

Chernomor O, von Haeseler A, Minh BQ. Terrace aware data structure for phylogenomic inference from supermatrices. *Systematic Biology* 2016;**65**:997–1008.

Conroy CJ, Cook JA. Molecular systematics of a Holarctic rodent (*Microtus*: Muridae). *Journal of Mammalogy* 2000;**81**:344–59.

Cooper A, Turney C, Hughen KA *et al.* Abrupt warming events drove Late Pleistocene Holarctic megafaunal turnover. *Science* 2015;**349**:602–6.

Cuenca-Bescós G, Straus LG, Morales MRG *et al.* The reconstruction of past environments through small mammals: from the Mousterian to the Bronze Age in El Miron Cave (Cantabria, Spain). *Journal of Archaeological Science* 2009;**36**:947–55.

Dabney J, Knapp M, Glocke I *et al.* Complete mitochondrial genome sequence of a Middle Pleistocene cave bear reconstructed from ultrashort DNA fragments. *Proceedings of the National Academy of Sciences of the United States of America* 2013;**110**:15758–63.

Danecek P, Bonfield JK, Liddle J *et al.* Twelve years of SAMtools and BCFtools. *GigaScience* 2021;**10**:giab008.

Depaulis F, Orlando L, Hanni C. Using classical population genetics tools with heterochroneous data: time matters! *PLoS One* 2009;**4**:e5541.

Discamps E, Royer A. Reconstructing palaeoenvironmental conditions faced by Mousterian hunters during MIS 5 to 3 in southwestern France: a multi-scale approach using data from large and small mammal communities. *Quaternary International* 2017;**433**:64–87.

Doan K, Niedziałkowska M, Stefaniak K *et al.* Phylogenetics and phylogeography of red deer mtDNA lineages during the last 50 000 years in Eurasia. *Zoological Journal of the Linnean Society* 2022;**194**:431–56.

Drummond AJ, Suchard MA, Xie D *et al.* Bayesian phylogenetics with BEAUti and the BEAST 1.7. *Molecular Biology and Evolution* 2012;**29**:1969–73.

Fedorov V, Goropashnaya A, Jarrell GH *et al.* Phylogeographic structure and mitochondrial DNA variation in true lemmings (*Lemmus*) from the Eurasian Arctic. *Biological Journal of the Linnean Society* 1999;**66**:357–71.

Fernández-García M, López-García JM, Lorenzo C. Palaeoecological implications of rodents as proxies for the Late Pleistocene-Holocene environmental and climatic changes in northeastern Iberia. *Comptes Rendus Palevol* 2016;**15**:707–19.

Galewski T, Tilak M, Sanchez S *et al.* The evolutionary radiation of Arvicolinae rodents (voles and lemmings): relative contribution of nuclear and mitochondrial DNA phylogenies. *BMC Evolutionary Biology* 2006;**6**:80.

Garcia-Ibaibarriaga N, Rofes J, Bailon S *et al.* A palaeoenvironmental estimate in Askondo (Bizkaia, Spain) using small vertebrates. *Quaternary International* 2015;**364**:244–54.

García-Morato S, Domínguez-García AC, Sevilla P *et al.* The last 20,000 years of climate change in the Iberian Peninsula characterized by the small-mammal assemblages. *Palaeogeography Palaeoclimatology Palaeoecology* 2024;**655**:112545.

García-Rodríguez O, Hardouin EA, Pedreschi D *et al.* Contrasting patterns of genetic diversity in European mammals in the context of glacial refugia. *Diversity* 2024;**16**:611.

Ginolhac A, Rasmussen M, Gilbert MTP *et al.* mapDamage: testing for damage patterns in ancient DNA sequences. *Bioinformatics* 2011;**27**:2153–5.

Gubányi A, Dudich A, Stollmann A *et al.* Distribution and conservation management of the root vole (*Microtus oeconomus*) populations along the Danube in Central Europe (Rodentia: Arvicolinae). *Lynx, n.s. (Praha)* 2009;**40**:29–42.

Helmens KF. The Last Interglacial–Glacial cycle (MIS 5–2) re-examined based on long proxy records from central and northern Europe. *Quaternary Science Reviews* 2014;**86**:115–43.
Herman JS, McDevitt AD, Kawałko A *et al.* Land-bridge calibration of molecular clocks and the post-glacial colonization of Scandinavia by the Eurasian field vole. *PLoS One* 2014;**9**:e103949.
Holling CS. Resilience and stability of ecological systems. *Annual Review of Ecology and Systematics* 1973;**4**:1–23.
Horn S. Target enrichment via DNA hybridization capture. *Ancient DNA: Methods and Protocols* 2012;**840**:177–88.
Hu A, Meehl GA, Otto-Bliesner BL *et al.* Influence of Bering Strait flow and North Atlantic circulation on glacial sea-level changes. *Nature Geoscience* 2010;**3**:118–21.
Iwasa M, Kostenko V, Frisman L *et al.* Phylogeography of the root vole *Microtus oeconomus* in Russian far east: a special reference to comparison between Holarctic and Palaearctic voles. *Mammal Study* 2009;**34**:123–30.
Jaarola M, Martinkova N, Gunduz I *et al.* Molecular phylogeny of the speciose vole genus *Microtus* (Arvicolinae, Rodentia) inferred from mitochondrial DNA sequences. *Molecular Phylogenetics and Evolution* 2004;**33**:647–63.
Kalyaanamoorthy S, Minh BQ, Wong TKF *et al.* ModelFinder: fast model selection for accurate phylogenetic estimates. *Nature Methods* 2017;**14**:587–9.
Kass RE, Raftery AE. Bayes factors. *Journal of the American Statistical Association* 1995;**90**:773–95.
Katoh K, Standley DM. MAFFT multiple sequence alignment software version 7: improvements in performance and usability. *Molecular Biology and Evolution* 2013;**30**:772–80.
Krokhmal' O, Rekovets L, Kovalchuk O. An updated biochronology of Ukrainian small mammal faunas of the past 1.8 million years based on voles (Rodentia, Arvicolidae): a review. *Boreas* 2021;**50**:619–30.
Krokhmal' O, Rekovets L, Kovalchuk O. Biochronological scheme of the Quaternary of the south of Eastern Europe and its substantiation based on arvicoline teeth morphometrics. *Quaternary International* 2023;**674-675**:5–17.
Kryštufek B, Shenbrot GI. *Voles and Lemmings (Arvicolinae) of the Palaearctic Region*. University of Maribor: University Press, 2022.
Lanfear R, Calcott B, Ho SY *et al.* Partitionfinder: combined selection of partitioning schemes and substitution models for phylogenetic analyses. *Molecular Biology and Evolution* 2012;**29**:1695–701.
Laplana C, Sevilla P, Blain H-A *et al.* Cold-climate rodent indicators for the Late Pleistocene of Central Iberia: new data from the Buena Pinta Cave (Pinilla del Valle, Madrid Region, Spain). *Comptes Rendus Palevol* 2016;**15**:696–706.
Larsson A. AliView: a fast and lightweight alignment viewer and editor for large datasets. *Bioinformatics* 2014;**30**:3276–8.
Lartillot N, Philippe H. A Bayesian mixture model for across-site heterogeneities in the amino-acid replacement process. *Molecular Biology and Evolution* 2004;**21**:1095–109.
Lemanik A, Baca M, Wertz K *et al.* The impact of major warming at 14.7 ka on environmental changes and activity of Final Palaeolithic hunters at a local scale (Orawa-Nowy Targ Basin, Western Carpathians, Poland). *Archaeological and Anthropological Sciences* 2020;**12**:66.
Li H, Durbin R. Fast and accurate long-read alignment with Burrows-Wheeler transform. *Bioinformatics* 2010;**26**:589–95.
Ligvoet W, van Wijngaarden A. The colonization of the island of Noord-Beveland (the Netherlands) by the common vole *Microtus arvalis*, and its consequences for the root vole *M. oeconomus*. *Lutra* 1994;**37**:1–28.
Liljegren R. *Subfossila vertebratfynd från Skåne*. University of Lund, Department of Quaternary Geology. Report 8, 1975.
Lisiecki LE, Raymo ME. A Pliocene-Pleistocene stack of 57 globally distributed benthic δ18O records. *Paleoceanography* 2005;**20**:PA1003.
Lord E. Investigating the impacts of Late Pleistocene climate change on Arctic mammals using palaeogenomics. Ph.D. Thesis, Department of Zoology, Stockholm University, 2022.
Lord E, Feinauer IS, Soares AER *et al.* Genome analyses suggest recent speciation and postglacial isolation in the Norwegian lemming. *Proceedings of the National Academy of Sciences of the United States of America* 2025;**122**:e2424333122.
Lord E, Marangoni A, Baca M *et al.* Population dynamics and demographic history of Eurasian collared lemmings. *BMC Ecology and Evolution* 2022;**22**:126. L.
Lorenzen ED, Nogues-Bravo D, Orlando L *et al.* Species-specific responses of Late Quaternary megafauna to climate and humans. *Nature* 2011;**479**:359–64.
Maricic T, Whitten M, Paabo S. Multiplexed DNA sequence capture of mitochondrial genomes using PCR products. *PLoS One* 2010;**5**:e14004.
Markova AK. Pleistocene Rodents of the Russian Plain. *Nauka, Moscow*, 1982;1–183. [in Russian].
Markova AK. Early Pleistocene small mammal faunas of the Eastern Europe. *Mededelingen Nederlands Instituut voor Toegepaste Geowetenschappen TNO* 1998;**60**:313–26.
Markova AK. Eastern European rodent (Rodentia, Mammalia) faunas from the Early-Middle Pleistocene transition. *Quaternary International* 2005;**131**:71–7.
Markova AK, Puzachenko AY. Middle Pleistocene small mammal faunas of Europe: evolution, biostratigraphy, correlations. *Geography, Environment, Sustainability* 2018;**11**:21–38.
Marková S, Horníková M, Lanier HC *et al.* High genomic diversity in the bank vole at the northern apex of a range expansion: the role of multiple colonizations and end-glacial refugia. *Molecular Ecology* 2020;**29**:1730–44.
Martínková N, Moravec J. Multilocus phylogeny of arvicoline voles (Arvicolini, Rodentia) shows small tree terrace size. *Folia Zoologica* 2012;**61**:254–67.
Matzke NJ. BioGeoBEARS: BioGeography with Bayesian (and likelihood) evolutionary analysis in R scripts. R package, 2013. https://github.com/nmatzke/BioGeoBEARS
Maul LC, Markova AK. Similarity and regional differences in Quaternary arvicolid evolution in Central and Eastern Europe. *Quaternary International* 2007;**160**:81–99.
Meyer M, Kircher M. Illumina sequencing library preparation for highly multiplexed target capture and sequencing. *Cold Spring Harbor Protocols* 2010;**2010**:pdb prot5448.
Milne I, Bayer M, Stephen G *et al.* Tablet: visualizing next-generation sequence assemblies and mappings. *Plant Bioinformatics: Methods and Protocols* 2016;**1374**:253–68.
Nadachowski A. Origin and history of the present rodent fauna in Poland based on fossil evidence. *Acta Theriologica* 1989;**34**:37–53.
Nguyen LT, Schmidt HA, von Haeseler A *et al.* IQ-TREE: a fast and effective stochastic algorithm for estimating maximum-likelihood phylogenies. *Molecular Biology and Evolution* 2015;**32**:268–74.
Niedziałkowska M, Doan K, Górny M *et al.* Winter temperature and forest cover have shaped red deer distribution in Europe and the Ural Mountains since the Late Pleistocene. *Journal of Biogeography* 2021;**48**:147–59.
Niedziałkowska M, Górny M, Gornia J *et al.* Impact of global environmental changes on the range contraction of Eurasian moose since the Late Pleistocene. *The Science of the Total Environment* 2024;**957**:177235.
Palkopoulou E, Baca M, Abramson NI *et al.* Synchronous genetic turnovers across Western Eurasia in Late Pleistocene collared lemmings. *Global Change Biology* 2016;**22**:1710–21.
Popova L, Veklych Y, Kovalchuk O *et al.* Within the boundaries of the Dnipro ice lobe: biotic dynamics in the Middle Dnipro area (Ukraine) during deglaciation and postglacial stages. *Journal of Quaternary Science* 2025;**40**:53–70.
Quinlan AR, Hall IM. BEDTools: a flexible suite of utilities for comparing genomic features. *Bioinformatics* 2010;**26**:841–2.
R Core Team. 2022. R: a language and environment for statistical computing. Vienna, Austria: R Foundation for Statistical Computing. https://www.R-project.org/.
Rabiniak E, Rekovets L, Kovalchuk O *et al.* Hares from the Late Pleistocene of Ukraine: a phylogenetic analysis and the status of *Lepus tanaiticus* (Mammalia, Lagomorpha). *Biologia* 2024;**79**:87–99.
Rabiniak E, Rekovets L, Stewart JR *et al.* Late Pleistocene and Holocene pikas (Mammalia, Lagomorpha) from Europe and the validity of *Ochotona spelaea*: new insights based on mtDNA analysis. *Palaeontologia Electronica* 2023;26.1.a3.

Ramsey CB. Bayesian analysis of radiocarbon dates. *Radiocarbon* 2009;**51**:337–60. [Database].

Rasmussen SO, Bigler M, Blockley SP *et al.* A stratigraphic framework for abrupt climatic changes during the Last Glacial period based on three synchronized Greenland ice-core records: refining and extending the INTIMATE event stratigraphy. *Quaternary Science Reviews* 2014;**106**:14–28.

Rausch RL. A review of the distribution of Holarctic recent mammals. *Faculty Publications from the Harold W. Manter Laboratory of Parasitology* 1963;**518**:29–43.

Reimer PJ, Austin WEN, Bard E *et al.* The Intcal20 northern hemisphere radiocarbon age calibration curve (0-55 Cal Kbp). *Radiocarbon* 2020;**62**:725–57.

Rekovets L. Small mammals from the Anthropocene of the southern part of East Europe. *Naukova Dumka, Kiev*, 1994, 1–371. [in Russian].

Rekovets L, Nadachowski A. Pleistocene voles (Arvicolidae) of the Ukraine. *Paleontologia i Evolutio* 1995;**28–29**:145–245.

Robovský J, Řičánková V, Zrzavý J. Phylogeny of Arvicolinae (Mammalia, Cricetidae): utility of morphological and molecular data sets in a recently radiating clade. *Zoologica Scripta* 2008;**37**:571–90.

Ronquist F, Teslenko M, van der Mark P *et al.* MrBayes 3.2: efficient Bayesian phylogenetic inference and model choice across a large model space. *Systematic Biology* 2012;**61**:539–42.

Royer A, Laroulandie V, Bailon S *et al.* Chapitre 3. Des restes de faune aux paléoenvironnements de Peyrazet. In: Langlais M, Laroulandie V (ed.), *La Grotte-abri de Peyrazet (Creysse, Lot, France) au Magdalénien: Originalité fonctionnelle d'un habitat des derniers chasseurs de rennes du Quercy.* CNRS, Supplément à Gallia Préhistoire 2021;**43**:35–48.

Royer A, Montuire S, Legendre S *et al.* Investigating the influence of climate changes on rodent communities at a regional-scale (MIS 1-3, Southwestern France). *PLoS One* 2016;**11**:e0145600.

Schubert M, Lindgreen S, Orlando L. AdapterRemoval v2: rapid adapter trimming, identification, and read merging. *BMC Research Notes* 2016;**9**:88.

Seierstad IK, Abbott PM, Bigler M *et al.* Consistently dated records from the Greenland GRIP, GISP2 and NGRIP ice cores for the past 104 ka reveal regional millennial-scale $\delta^{18}O$ gradients with possible Heinrich event imprint. *Quaternary Science Reviews* 2014;**106**:29–46.

Sese C, de la Rasilla M, Matias ED. The micromammals (Eulipotyphla, Chiroptera, Rodentia and Lagomorpha) from the Late Pleistocene site of the El Sidron cave (Asturias). *Estudios Geologicos-Madrid* 2018;**74**.

Shenbrot GI, Krasnov BR. *An Atlas of the Geographic Distribution of the Arvicoline Rodents of the World (Rodentia, Muridae, Arvicolinae)*. Sofia, Bulgaria: Pensoft Publishers, 2005.

Stefaniak K, Kovalchuk O, Marciszak A *et al.* Environmental conditions across Poland during the Eemian Interglacial reconstructed from vertebrate remains. *Acta Geologica Polonica* 2023;**73**:379–410.

Stewart JR, Lister AM, Barnes I, Dalen L. Refugia revisited: individualistic responses of species in space and time. *Proceedings of the Royal Society B-Biological Sciences* 2010;**277**:661–71.

Stojak J, McDevitt AD, Herman JS *et al.* Post-glacial colonization of eastern Europe from the Carpathian refugium: evidence from mitochondrial DNA of the common vole *Microtus arvalis*. *Biological Journal of the Linnean Society* 2015;**115**:927–39.

Svenning J-C, Lemoine RT, Bergman J *et al.* The Late-Quaternary megafauna extinctions: patterns, causes, ecological consequences and implications for ecosystem management in the Anthropocene. *Cambridge Prisms. Extinction* 2024;**2**:e5.

Thissen JBM, Bekker DL, Spreitzer K *et al.* The distribution of the Pannonic root vole (*Microtus oeconomus mehelyi* Ehik, 1928) in Austria. *Lutra* 2015;**58**:3–22.

Velichko AA, Markova AK, Pevzner MA *et al.* The position of paleomagnetic epochs Matuyama-Brunhes in chronostratigraphical scale of East European continental deposits. *Doklady Akademii Nauk SSSR* 1983;**269**:1147–50.

Xie W, Lewis PO, Fan Y *et al.* Improving marginal likelihood estimation for Bayesian phylogenetic model selection. *Systematic Biology* 2011;**60**:150–60.

Yu Y, Harris AJ, Blair C *et al.* RASP (Reconstruct Ancestral State in Phylogenies): a tool for historical biogeography. *Molecular Phylogenetics and Evolution* 2015;**87**:46–9.

Zagorodnyuk IV. Kariotypic variability and systematics of the Arvicolini (Rodentia). Communication 1. Species and chromosomal numbers. *Vestnik Zoologii* 1990;**2**:26–37.